Functional Flight Test Report

For

Positive Systems' ADAR System 5500 Sensor

SN8 Linear

By

Lockheed Martin Space Operations – Stennis Programs

John C. Stennis Space Center, MS 39529-6000

For

Commercial Remote Sensing Program

National Aeronautics and Space Administration

John C. Stennis Space Center, MS 39529-6000

January 21, 2000

Prepared by:
Slawomir Blonski, Technical Lead
Kimberly Macey, Technical Staff
Christopher Schera, Technical Staff
Lockheed Martin CRSP

Approved by:	Signature	Date
Robert Ryan, Manager Lockheed Martin CRSP		

Concurrence:	Signature	Date
Tom Stanley, Technical Monitor NASA CRSP		

Table of Contents

List of Figures

Summary

This report describes results of the functional flight test conducted with the Positive Systems' ADAR 5500 sensor system (serial number 8, linear configuration) near Winslow, Arizona on June 30 and July 1, 1999. The in-flight test is one component of the NASA Scientific Data Purchase (SDP) Validation and Verification (V&V) process. It allows to measure characteristics of the entire sensor system affected by both performance of the sensor during a flight and post-flight image processing. The following characteristics were analyzed: changes of dark digital numbers (DN's), radiometric linearity, signal-to-noise ratio (SNR), spatial resolution, and geolocation accuracy. The measured characteristics were compared with the image product specifications defined in the Positive Systems' SDP contract. Dependence of the dark DN's on several factors was analyzed, but no significant correlation was found. However, the observed changes in dark DN's were relatively small, which justifies usage of a constant value in the dark DN subtraction procedure during post-processing. Dependence of measured at-sensor, in-band radiance (in arbitrary units) on measured in-band ground reflectance is very well described by a linear function – The sensor fulfills the linearity requirement. Measured SNR values lower than the contract specifications, but accuracy of that test was possibly affected by non-uniformity of the employed gray-scale panels. The SNR values are generally sufficiently high for most applications. SNR can also be improved during standard flights by using longer exposure times. Full width at half maximum (FWHM) of an edge response derived line spread function was used as a measure of spatial resolution. FWHM was generally smaller than twice the ground sample distance (GSD), in agreement with the contract specifications. Accuracy of the geolocation information, which is provided for the particular images in a metadata file, was found to meet contract requirements as well.

A set of images acquired during the functional flight test was also used by Positive Systems to create a georeferenced mosaic image. Analysis of image quality and geolocation accuracy of the mosaic were conducted and presented separately. The same set of images was also used to test procedures developed for validation of image products created after standard flights scheduled under the SDP program. It was found that the procedures, which are described in this report, could be applied in the validation process.

The main recommendation from analysis of this functional flight test is that an exceptional care should be taken about size and uniformity of the gray-scale panels used in such in-flight testing. Both affect significantly tests of radiometric characteristics and spatial resolution.

Introduction

Positive Systems, Inc., of Whitefish, Montana uses its airborne ADAR System 5500 sensors to acquire multispectral remote sensing images delivered to NASA under the Scientific Data Purchase (SDP) program. Functional flight tests are one component part of the SDP Verification & Validation process. Other components include laboratory and standard flight characterization. These are covered in other reports. The functional flight test of the Positive Systems' ADAR 5500 sensor system with the serial number 8 (SN8) was conducted on June 30 and July 1, 1999 at the Hopi Reservation located southeast of Winslow, Arizona (see Appendix A and Appendix B). During the test, a six-step gray scale target was deployed on the ground at coordinates of 34° 51' 18.865" N latitude and 110° 39' 31.17" W longitude (see Figure 1) [MTL 1999]. Two independent teams, one from the MTL Systems, Inc., and the other from the NASA Stennis Space Center (Ground Reference Information Team, GRIT), measured spectral reflectance of the gray panels using calibrated spectroradiometers. A network of high-precision geodetic targets was also located at the test site. Geolocation of the targets was measured with Global Positioning System (GPS) survey equipment [Shingoitewa-Honanie and Jenner, 1998] to xx precision. During the first day of the test, the gray-scale target was overflown several times using two mutually perpendicular headings and four different altitudes. Using the different altitudes, images were acquired with ground sample distances (GSD) of 0.3, 0.5, 0.75, and 1 meter. During the second day, images were acquired in seven parallel flight lines over the geodetic target range with GSD of 0.75 meter. After the flights, Positive Systems processed all the images as described in Appendix C and created a georeferenced mosaic from the images acquired on the second day.

This documents describes results of in-flight testing of the following sensor system characteristics:

- Dark DN's
- Radiometric linearity
- Signal-to-noise ratio
- Spatial resolution
- Geolocation accuracy

The set of images acquired on the second day was also used to test procedures developed for validation of image products acquired during standard flights. The product validation procedures and results of their testing are described later in this document. Evaluation of geolocation accuracy of the mosaic image is presented in a separate report [LMSO 1999b].

Figure 1. Six-step gray scale target deployed at the test site near Winslow, Arizona.

Dark DN's

Dark images were aqcuired on the ground and in-flight at all the altitudes. At every altitude, two series of 10 images each were collected. Analysis was performed separately for each series. A histogram of DN distribution was created for each band of every image. All the histograms in one series were used to calculate an average histogram and its standard deviation. Examples of the average histograms for different spectral bands are shown in Figure 2.

The dark images were also used to calculate mean dark DN and its standard deviation for each series. Correlation of the mean dark DN's and the average histograms with such quantities as acquisition time, altitude, and temperature were examined. No clear dependency on time and altitude of the acquisition was observed. The only significant correlation was the one with temperature (see Figure 3). Mean dark DN's become smaller when temperature increases. This is inconsistent with the dark current properties of a Si: detector array. A possible explanation may be in thermal characteristics of the sensor electronics (such as amplifier offsets). Nevertheless, the mean dark DN's changed only between 7.3 and 9.4 for the entire observed temperature range. Such a small change justifies usage of a constant value of 8 (instead of a more precise value) in the dark DN subtraction applied by Positive Systems during post-processing: No significant radiometric error is introduced by the approximate process.

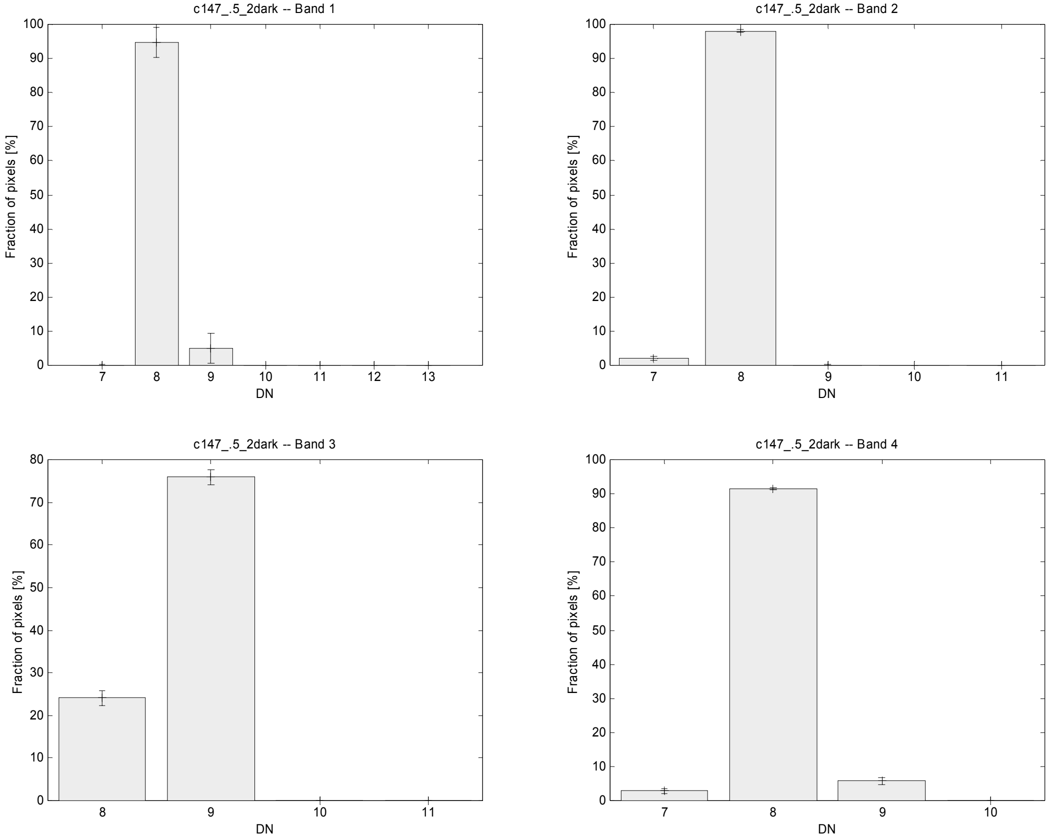

Figure 2. Mean histograms of dark DN distributions generated from images acquired at altitude suitable for 0.5 m GSD. Error bars indicate standard deviations.

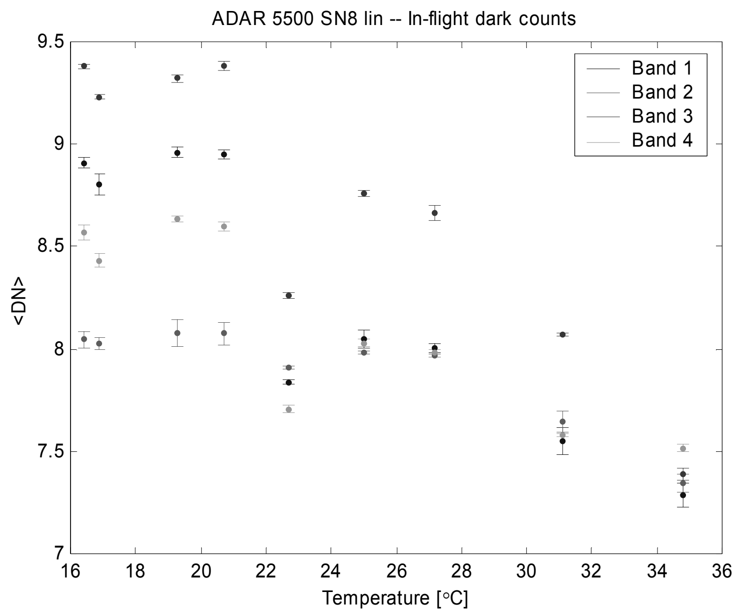

Figure 3. Dependence of mean dark DN's on temperature.

Radiometric linearity

Images of the six-step gray scale target were used for in-flight characterization of the sensor radiometric linearity (see Figure 4). Dependence of in-band at-sensor radiance on in-band ground reflectance was evaluated instead of comparison of the measured radiance with the one calculated from atmospheric radiative transfer models. The former is more closely related to the needs of scientists who are users of the commercially acquired images, while the latter is prone to many uncertainties inherent to the atmospheric modeling [Freedman 1999]. Dry atmospheric conditions of the Arizona test site may have contributed significantly to success of the performed analysis.

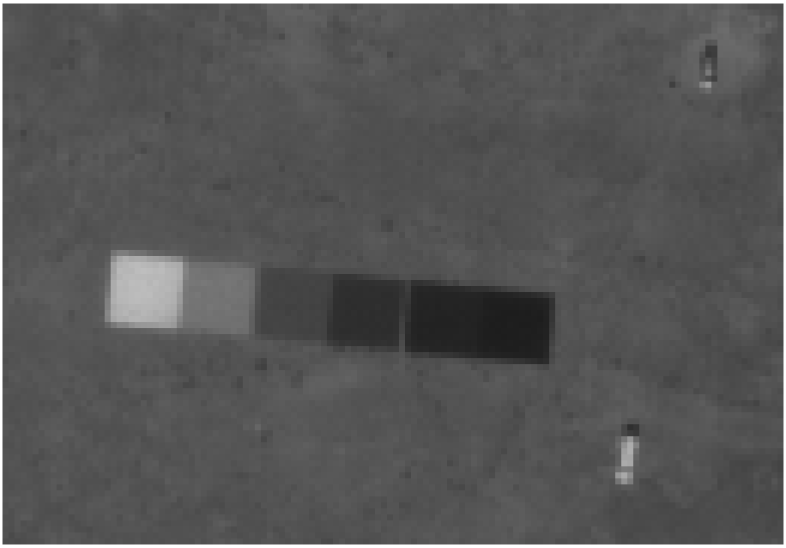

Figure 4. Image of the six-step gray scale target acquired by the ADAR 5500 sensor (band 3) with GSD of 0.75 m. Vehicles of the ground support team are visible in the right-side corners of the image (compare Figure 1).

Values of in-band radiance measured by the sensor (in arbitrary units) were extracted from the images. A rectangular region-of-interest (ROI) was selected for each panel area (see Figure 5), and mean and standard deviation of DN's for all the pixels belonging to the ROI were calculated. The calculations were performed for each band separately. Mean DN was used as the measure of radiance for a given panel, while standard deviation was used to estimate noise (see section *Signal-to-noise ratio*).

In-band reflectance of the gray panels was calculated from results of the ground measurements. While the measurements by the two teams produced slightly different results (see Figure 6), the spectra provided by MTL were used in the calculations of in-band reflectance. In-band reflectance ρ_k is defined here by the following equation:

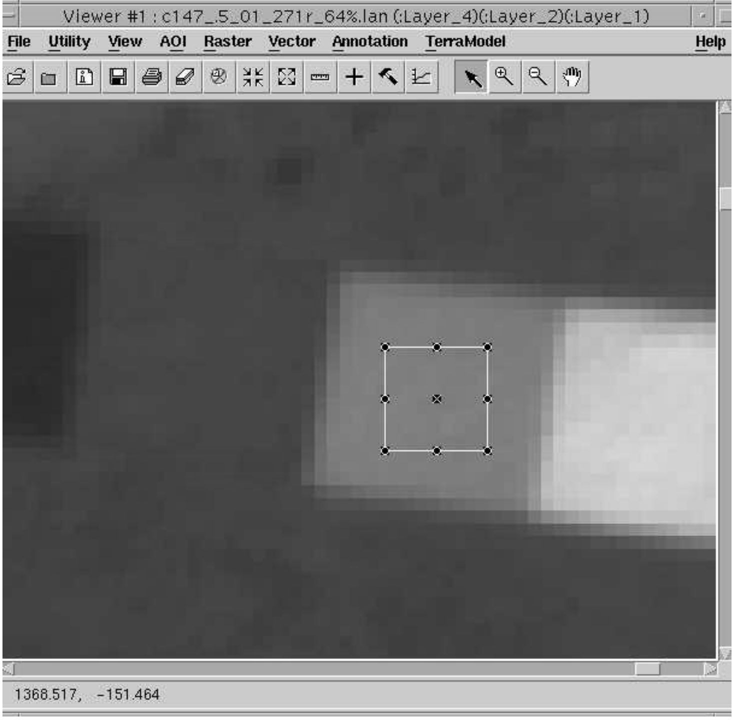

Figure 5. Region-of-interest selected for the radiometric analysis.

$$\rho_k = \frac{\int \rho(\lambda) R_k(\lambda) d\lambda}{\int R_k(\lambda) d\lambda}$$

where λ is the radiation wavelength, $\rho(\lambda)$ is the spectral reflectance of the panel surface and $R_k(\lambda)$ is the spectral response function of the k^{th} band of the sensor. Spectral response functions measured during characterization of the sensor in the Commercial Instrument Validation Laboratory were used in the calculations [LMSO 1999a]. Both integrals were evaluated numerically with integration limits from 400 nm to 950 nm and with the increment of 1 nm. To have both the reflectance spectrum and the spectral response sampled at the same wavelengths, the functions were interpolated with splines (see Figure 7).

Linear regression between in-band radiance and in-band reflectance was calculated using all the six gray panels from a single image. Gray-scale targets from different images were analyzed separately as the images were acquired at various times during the day under different solar illumination conditions. Examples of the main results of the linearity tests are shown in Figure 8. In all the cases studied, dependence of the radiance on the reflectance is decidedly linear as specified in the requirements.

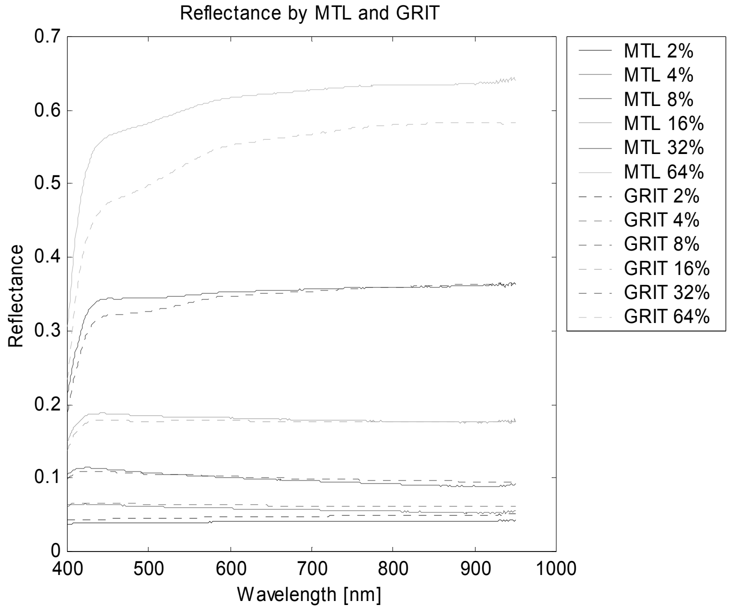

Figure 6. Reflectance spectra of the gray panels measured on June 30, 1999 by the MTL and GRIT teams.

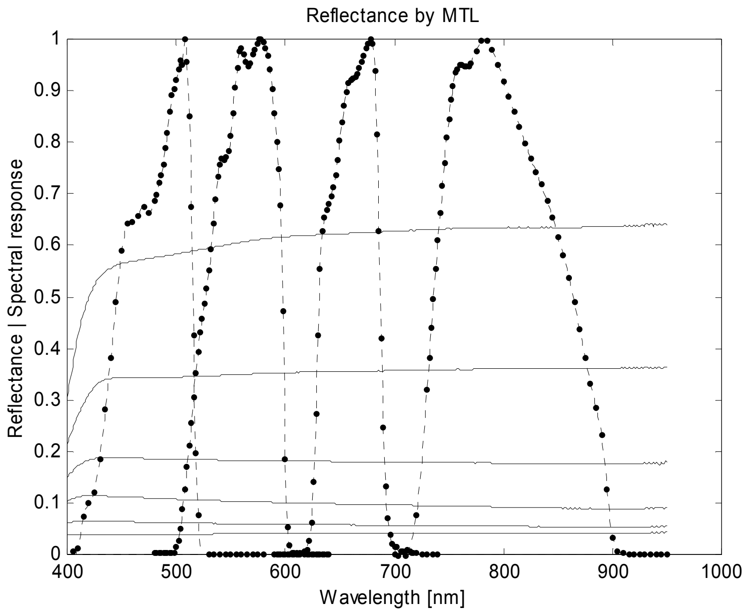

Figure 7. Reflectance spectra of the gray panels and spectral response of the ADAR 5500 SN8 sensor used in the calculations of the in-band reflectance.

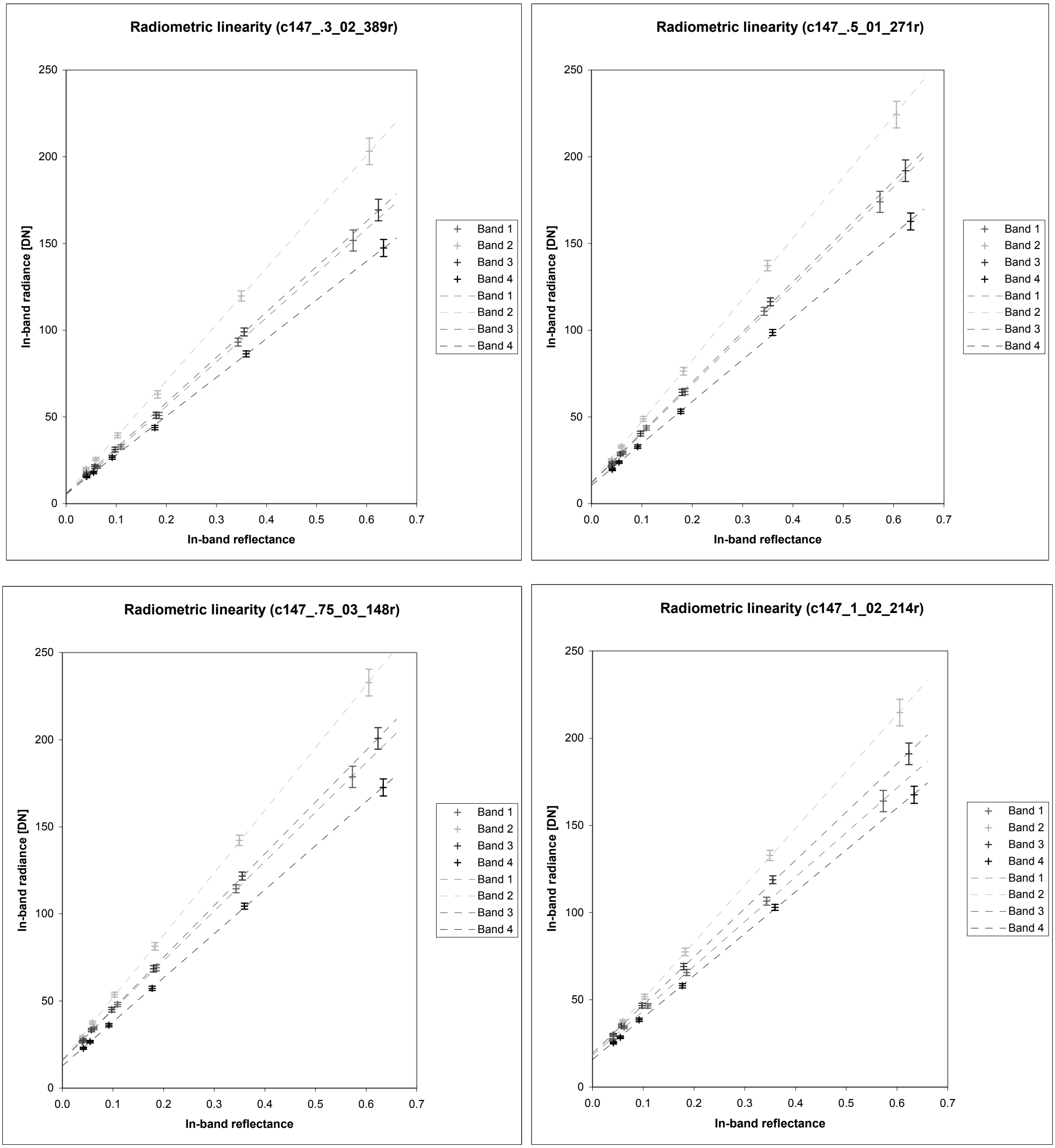

Figure 8. Examples of dependence of measured in-band radiance (in arbitrary units) on ground in-band reflectance. GSD equals 0.3 m (top left), 0.5 m (top right), 0.75 m (bottom left), and 1 m (bottom right).

Signal-to-noise ratio

Mean DN's were divided by standard deviations to calculate values of signal-to-noise ratio (SNR) for the gray panels. Examples of dependence of the calculated SNR's on in-band reflectance are presented in Figure 9. SNR monotonically increases with increasing reflectance (as well as radiance), as expected for a photon-limited sensor [LMSO 1999a]. For the most reflective panel, this relation is clearly violated as a result of radiometric non-uniformity of the surface (compare Figure 1). As the entire acquisition of the images on June 30, 1999 lasted for a considerable length of time, solar zenith angle also changed significantly. The solar zenith angles were calculated using the MODTRAN program and location/time data provided in the GPS file. See section V of the Customer Data Sheet in Appendix C for more information about this file. Images, for which the six-step gray scale targets were analyzed, were acquired with the solar zenith angle of 13.8, 19.7, 26.4, and 35.4 degrees. These images have GSD of 0.75, 1, 0.5, and 0.3 m, respectively. The images with GSD of 0.5 m were collected under illumination conditions that are the closest to the solar zenith angle of 30° defined in the requirements. For that image, SNR is about 60 for surface with 20% reflectance. The SNR specification for this tarp is that the SNR be greater than 90. While this number is lower than the requirement, there is significant uncertainty in this in-flight SNR measurement affected by sizes of the gray panels and especially their uniformity. Moreover, the ADAR 5500 sensor allows for selection of exposure times used in acquisition of the images. During the functional flight test, short exposure times were used to minimize image saturation in the gray-scale target area. However, during standard flights, images can be acquired using longer exposure times, which will increase SNR at a potential cost of more extensive saturation.

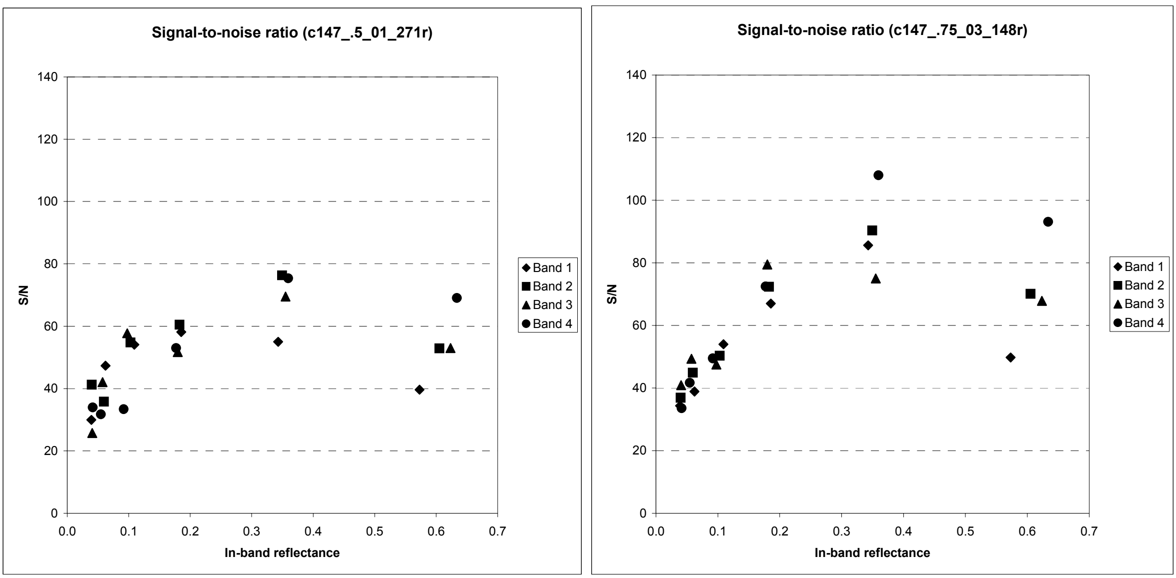

Figure 9. Examples of dependence of signal-to-noise ratios on in-band reflectance with solar zenith angle of 26.4° (left) and 13.8° (right).

Spatial resolution

Full Width at Half Maximum (FWHM) of a line spread function (LSF) is used as a measure of spatial resolution of the sensor system. Line spread functions are derived from edge responses by differentiation. There are three edges in the six-step gray scale target between pairs of adjacent panels. The edge between the most reflective panels was selected for the analysis because only that one provided sufficient contrast. The edge responses were measured and analyzed using a modified knife-edge technique [Tzannes and Mooney 1995]. A rectangular region containing a slightly tilted horizontal or vertical edge was extracted from an image of the gray panels as shown in Figure 10.

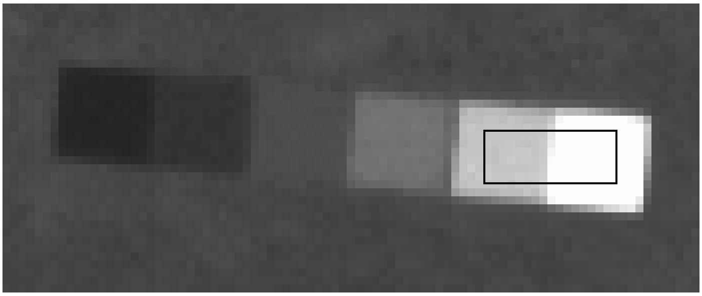

Figure 10. Rectangular edge-response region selected from the gray panels for analysis of spatial resolution.

In such a region, each line across the edge forms an approximate edge response. Exact edge responses (in the direction perpendicular to the edge) are obtained when distances are additionally scaled by cosine of the tilt angle. To avoid numerical differentiation, which can enhance noise, a differentiable function is fitted to the edge responses. In the approach presented in this report, the function has the sigmoidal form (known also from the Fermi distribution):

$$f(x) = \frac{a}{1 + \exp\left[\dfrac{x-b}{c}\right]}$$

However, for each edge response in the selected region, position of the edge (b) is different because of the tilt. Shape of the edge causes that all the positions b are located on a straight line. Therefore, the fitting is performed for all the edge responses simultaneously using the formula:

$$e_i(x) = \frac{a}{1 + \exp\left[\dfrac{x - b_1 i - b_2}{c}\right]} + d$$

The parameters a, b_1, b_2, c, and d are common for all the edge responses, while the difference in the edge position is introduced by the index (i). Tangent of the tilt angle is equal to the absolute value of the parameter b_1. Figure 11 shows an example of the edge responses and the best fit to them using the sigmoidal functions.

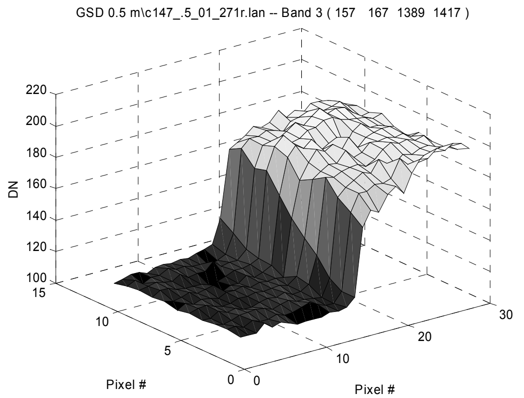

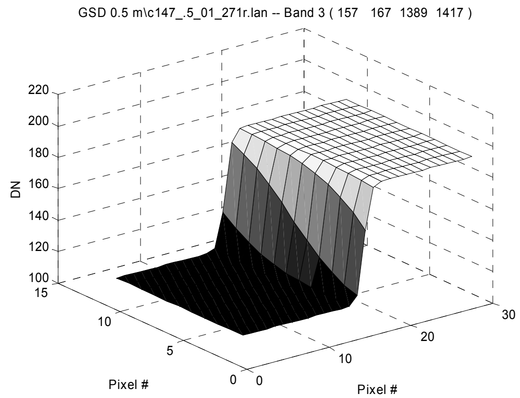

Figure 11. An example of measured edge responses (left) and the best fit to them with sigmoidal functions (right).

Finding the parameters b_1 and b_2 is equivalent to shifting the edge responses to a single reference location so that all the edge points are aligned. Superimposing all the shifted edge responses creates a new one with a finer spatial sampling (see Figure 12). This illustrates how the modifications to the knife-edge method allow to overcoming the main difficulty in applying such a method for digital sensors which employ discrete sampling of the image space.

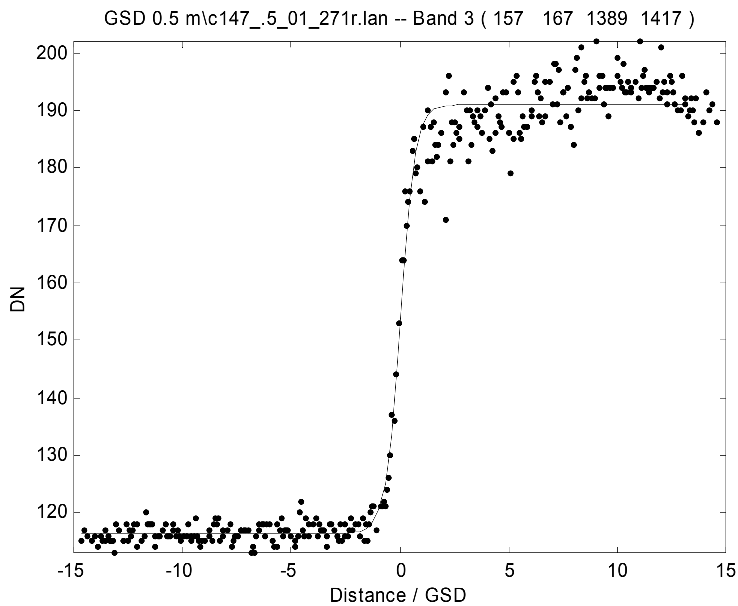

Figure 12. Superimposed edge responses and the fitted sigmoidal function.

The sigmoidal function with parameters obtained from the best fit is differentiated analytically to derive the LSF and its FWHM (see Figure 13). The LSF is sampled with a sufficient rate to avoid aliasing in the digital Fourier transform process, and the FFT algorithm is applied to it to compute the system modulation transfer function (MTF). Nyquist frequency is also marked on the MTF plot shown in Figure 14.

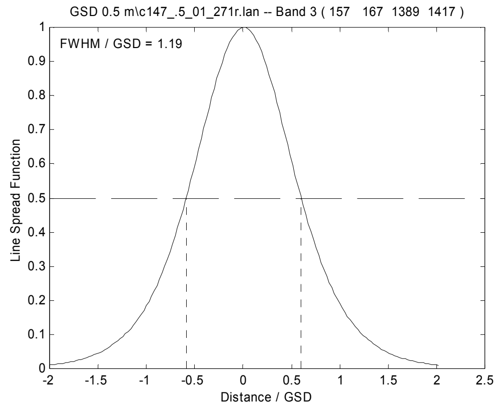

Figure 13. Line spread function derived from the edge responses shown in Figure 11 and Figure 12.

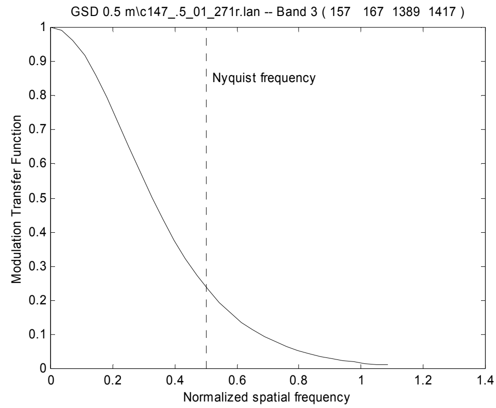

Figure 14. MTF estimated from the LSF shown in Figure 13.

Spatial resolution was analyzed for all the images of the gray scale target acquired during the first day of the functional flight test. The results for both cross-track and along-track direction are shown together in Figure 15. Some dependency of the results on the GSD can be noticed, but generally, FWHM is smaller than twice the GSD. This means that the tested sensor system, which includes both the ADAR 5500 SN8 sensor itself and the post-processing procedures, meets the requirements for spatial resolution.

Geolocation accuracy

Approximate geolocation of a center point of each image is provided in the GPS file. Accuracy of those data was evaluated by measuring twice the distance between the image center point and another point, which location is known with high accuracy. One measurement was based on distance (in pixels) between the points and an estimated value of GSD (based on ground elevation and aircraft altitude). The other measurement was based on the earth's radius and the difference between geographic coordinates (latitude and longitude) of the points. The geodetic targets became the points with accurate geolocation. Seventeen images of the geodetic targets were identified. An example of such an image is shown in Figure 16: the target is visible as white cross on black background. Pixel coordinates of the intersection of the cross arms were determined and used in the calculations using the following formula:

$$\Delta d = \left| \alpha(h-h_0)\sqrt{\left(\frac{i_{\max}}{2}-i_0\right)^2+\left(\frac{j_{\max}}{2}-j_0\right)^2} - R\sqrt{\left[(\lambda-\lambda_0)\cos\left(\frac{\vartheta+\vartheta_0}{2}\right)\right]^2+(\vartheta-\vartheta_0)^2} \right|$$

where: Δd – distance error

α – instantaneous field of view of the sensor

h – aircraft altitude

h_0 – elevation of the geodetic target

R – earth's radius

$i_{\max}, j_{\max}$ – image size

i_0, j_0 – pixel indices of the geodetic target on the image

λ, ϑ – longitude and latitude of the image center

λ_0, ϑ_0 – longitude and latitude of the geodetic target

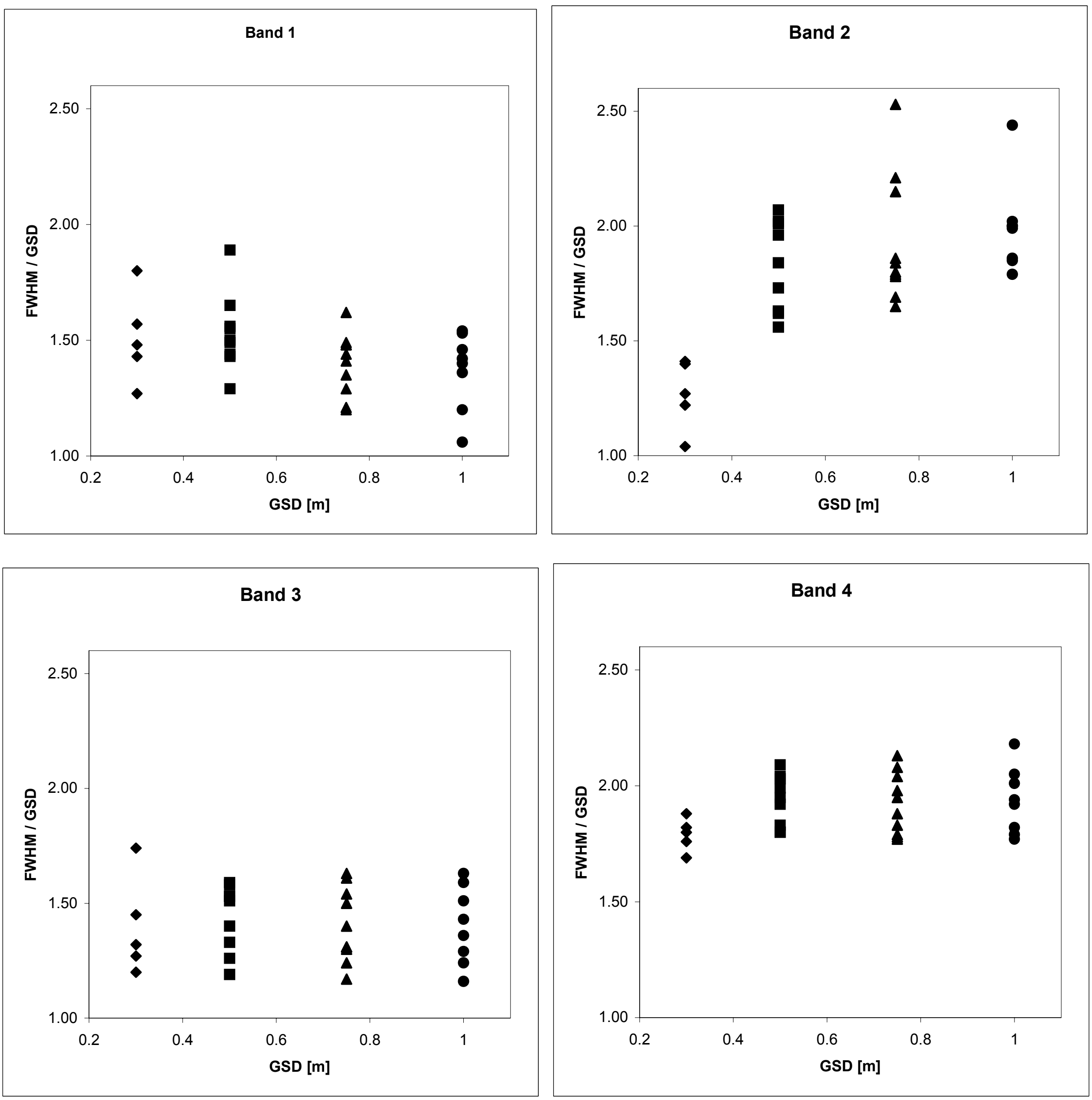

Figure 15. Ratios of FWHM to GSD determined in tests of spatial resolution based on measurements of edge responses.

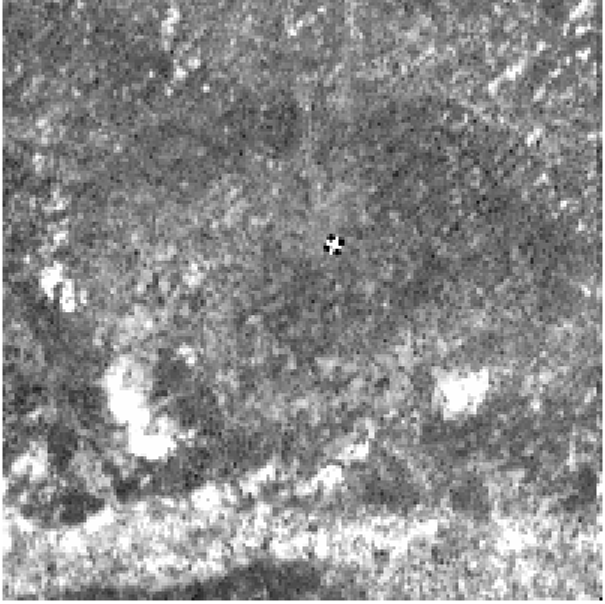

Figure 16. Image of a geodetic target.

Results of the calculations of geolocation accuracy are shown in Figure 17. The sensor system meets requirements for the geolocation accuracy because about 90% of the points (15 of 17) have location errors smaller than 100 m. The mean error is 49 m with standard deviation of 37 m.

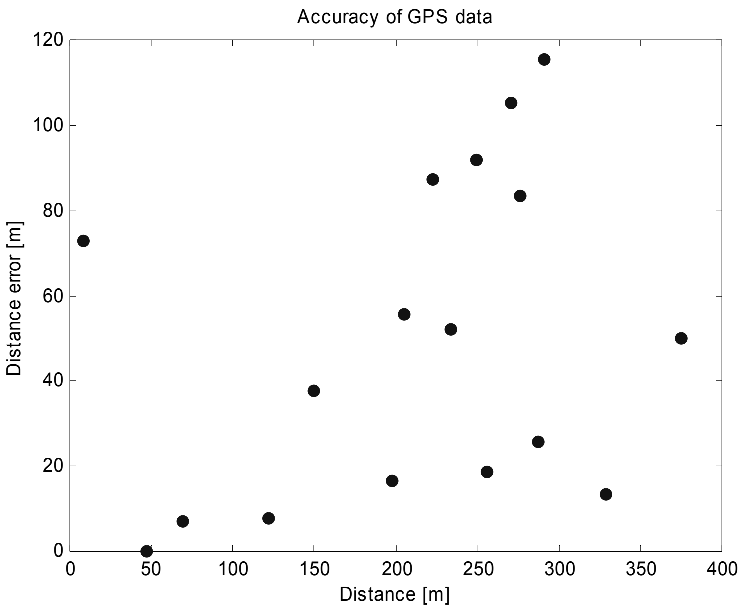

Figure 17. Distance errors measured during evaluation of geolocation accuracy.

Tests of standard flight validation

Verification and Validation (V&V) activities for imagery acquired under the NASA Scientific Data Purchase program using the Positive Systems' ADAR System 5500 sensors consist of three parts:

- Laboratory characterization of the sensors
- In-flight testing of sensor performance
- Validation of image products

Initial tests are performed in a laboratory environment to characterize spectral, spatial and radiometric response of every ADAR System 5500 sensor used in the Data Purchase program. Results of such tests have already been reported (see, for example, LMSO 1999a). Further characterization comes from functional flight tests during which the sensors acquire images over well-characterized spatial, radiometric, and geodetic targets. Previous sections of this report describe results of such in-flight testing. Finally, all images produced during standard flights, scheduled under the Data Purchase program, are validated to ensure consistent quality of image acquisition and post-processing. Images acquired on the second day of the testing at the Hopi site can be considered as a model of imagery collected during a standard flight. Therefore, these images were used to test procedures used for validation of image products delivered to NASA by Positive Systems under the name *IM-R1I-55, Imagery with Post-Flight Correction*. Results of applying the validation procedure to this set of images are presented later in this section. The following paragraphs present the procedure as it may be described in work instructions.

The objective is to ensure that general image quality, overlaps between images, spectral (band-to-band) registration, and possibly percentage of cloud cover as well as spatial resolution, conform to the contract requirements. Geographic coverage of a complete data set is verified during the Verification of Commercial Data Shipments process (see CRSP-WI-22).

General Image Quality

The images are evaluated to ensure proper sensor operation during the standard flight (i.e., no shutter failures, no significant amount of "bad" pixels, adequate settings of exposure time, etc.). The evaluation is based on distributions of DN's in each band of an image. As it would be extremely difficult for product validation personnel to generate and analyze interactively histograms of the DN's distributions for every image in a data set, the distributions are characterized by their first four moments (mean, standard deviation, skewness, and kurtosis) calculated using custom software (see Appendix E) and presented in a graphical form. Additional statistics, which are calculated for each band, include minimum DN, maximum DN, and percentage of pixels with the saturated DN value (the largest DN possible for a given quantization). Product validation personnel use the image statistics to detect anomalies in the image quality: Images with atypical statistics should be examined interactively using remote-sensing image processing software such as *ERDAS Imagine* or *ENVI*.

The statistics are calculated separately for each band of every image. For a given band, an image consists of M rows and N columns of pixels, where n_{ij} is the DN of the pixel located in the i^{th} row and the j^{th} column.

- Mean DN of an image is calculated using the following formula:

$$\bar{n} = \frac{1}{MN}\sum_{i=1}^{M}\sum_{j=1}^{N} n_{ij} .$$

- Standard deviation is a measure of width of the distribution of DN's, and it is defined by the following equation:

$$\sigma = \left[\frac{1}{MN-1}\sum_{i=1}^{M}\sum_{j=1}^{N}\left(n_{ij} - \bar{n}\right)^2\right]^{\frac{1}{2}} .$$

- Skewness is a measure of asymmetry of the distribution of DN's around the mean. The skewness of any perfectly symmetric distribution is zero. If the distribution of DN's is spread out more for DN's smaller than the mean, then skewness is negative. If the distribution of DN's is spread out more for DN's larger than the mean, then skewness is positive. The following formula is used to calculate skewness:

$$s = \frac{1}{\sigma^3}\left[\frac{1}{MN}\sum_{i=1}^{M}\sum_{j=1}^{N}\left(n_{ij} - \bar{n}\right)^3\right] .$$

- Kurtosis is a measure of how outlier-prone the distribution of DN's is. The kurtosis of the normal distribution is 3. Distributions that are more outlier-prone than the normal distribution have kurtosis greater than 3; distributions that are less outlier-prone have kurtosis less than 3. The following formula is used to calculate kurtosis:

$$k = \frac{1}{\sigma^4}\left[\frac{1}{MN}\sum_{i=1}^{M}\sum_{j=1}^{N}\left(n_{ij} - \bar{n}\right)^4\right] .$$

  Note: Some definitions of kurtosis subtract 3 from the computed value, so that the normal distribution has kurtosis of zero. This convention is not used in the presented calculations.
- Minimum DN is the smallest DN in an image.
- Maximum DN is the largest DN in an image.
- Saturation is measured as the percentage of pixels in an image that have DN equal to the maximum DN possible at a given quantization (for example, the maximum DN equals 255 for the 8-bit quantization).

While every image file in a data set is read during the statistics calculations, compatibility of the image file format is also validated. Moreover, the statistics may be instrumental in estimation of cloud cover percentage in a data set. Cloud cover is defined as the percentage of image surface covered by clouds, estimated on a per-scene basis for satellite data and on a per-site basis for aircraft data. Images with visible clouds will usually have all bands brighter than other images, while images with cloud shadows will usually have all bands darker than other images. Skewness and kurtosis may also be affected by clouds.

Overlaps between images

Overlaps are computed using custom software (see Appendix F) from a text file, which contains the GPS data recorded during the flight. Image center-point latitude and longitude are used, as are altitude and heading information. Ground elevation is acquired automatically from the U.S. Geological Survey's Digital Elevation Map (DEM) in the 1:250,000 scale with horizontal resolution of 100 m. The specified absolute horizontal accuracy of the DEM is 130 m, while the specified absolute vertical accuracy is ±30 m. The software employs trigonometric calculations to determine distances between image centers. Each distance is projected on a direction parallel (for endlap calculations) or perpendicular (for sidelap calculations) to a flight line, and is compared with a respective projection of image side lengths. Overlaps can be examined for flight lines in any orientation and order. For a given image, an endlap is calculated from the adjacent, subsequent image, and a sidelap is determined from the nearest, subsequent image on another flight line. Statistics of endlaps and sidelaps are generated for the entire data set. These statistics include mean, standard deviation, minimum, maximum, and percentage of overlaps smaller than a specified value.

Spectral Registration

Misregistration is calculated using custom software (see Appendix E) for every image in a data set. The calculations are performed for small sample regions (17 by 17 pixels) evenly distributed over the image area reduced by the size of overlaps. Approximately 200 to 400 regions are sampled in each image and used to calculate statistics of the spectral registration. For each region, two-dimensional (2D) cross-correlation is calculated for all the pairs of the spectral bands. Shift of a cross-correlation peak from the origin is used to measure the misregistration. Spatial resolution of determination of the peak position is enhanced from one pixel to 1/16 of a pixel by applying an interpolation based on the 2D fast Fourier transform (FFT). Statistics of the misregistration generated for an image include mean, standard deviation, and percentage of the sample regions with misregistration larger than a specified value. The percentage is also calculated for the entire data set. Only sample regions with misregistration smaller than two pixels are included in the calculations of statistics. When images with an extreme misregistration are detected, product validation personnel should use remote-sensing image processing software such as *ERDAS Imagine* or *ENVI* to interactively examine the images and evaluate impact of the misregistration on the image quality. Such images can be referred to a vendor for repeating the spectral registration processing and replacement.

Results

The entire set of 82 images acquired at the Hopi site in seven parallel flight lines on July 1, 1999 was used to test the validation procedures. The first part of image statistics is shown on graphs in Figure 18. For personnel conducting the image product validation, such graphs are presented interactively, with color coding of bands and ability to zoom in to identify particular images. The index included in Appendix D allows for precise identification of the images. Mean DN's indicate changes in solar illumination during the time of the flight. Effects of bi-directional reflectance may also be visible. The mean values are quite low, especially for band 1, which indicates that exposure times were slightly too short, but that was required by the high priority of avoiding saturation of images of the gray scale target. Standard deviations of DN distributions are also affected by that. Images that include the gray scale target have significantly larger skewness and kurtosis.

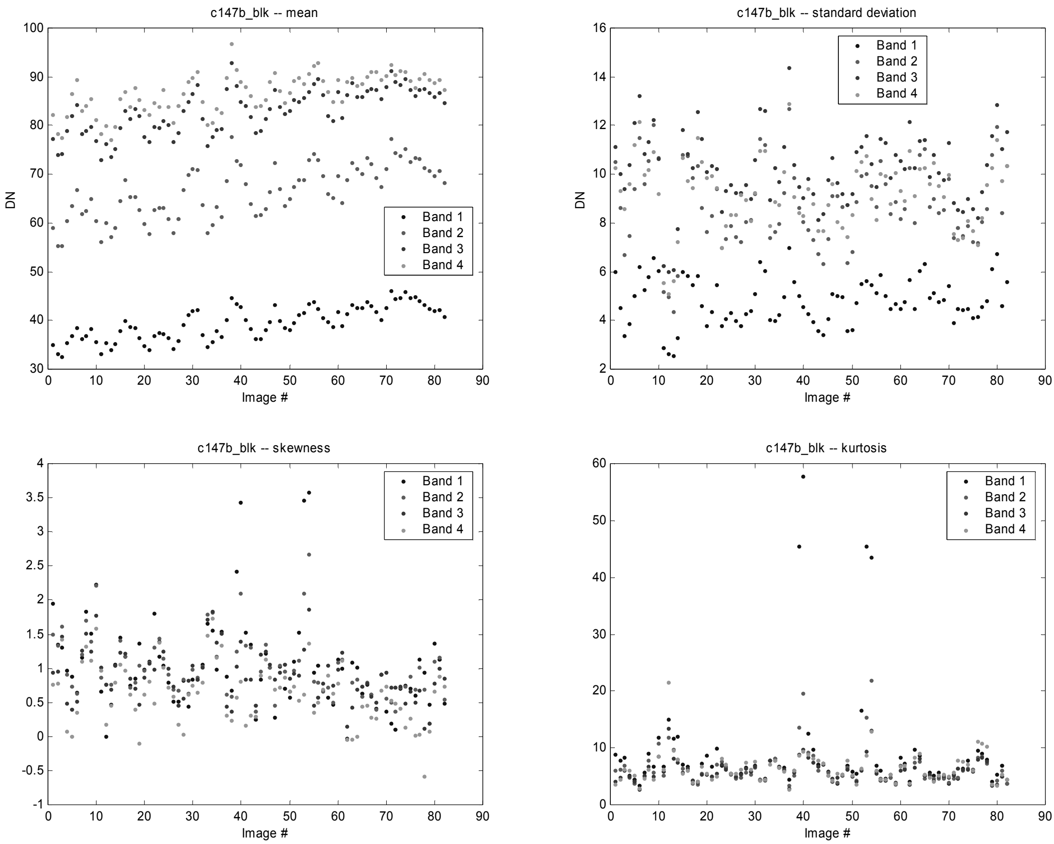

Figure 18. First four moments of the DN's distributions for every image in a data set: mean (top left), standard deviation (top right), skewness (bottom left), and kurtosis (bottom right)

Minimum and maximum DN's are shown in Figure 19. The graph of minimum DN's indicates that almost in every image there are pixels with DN equal to zero, at least in some bands. These pixels appear along edges of the images, in the corner areas. This is an artifact created during the spectral registration processing applied by Positive Systems: the images were not sufficiently trimmed to remove the “empty” pixels. The graph of maximum DN’s shows that only a small number of images have saturated pixels.

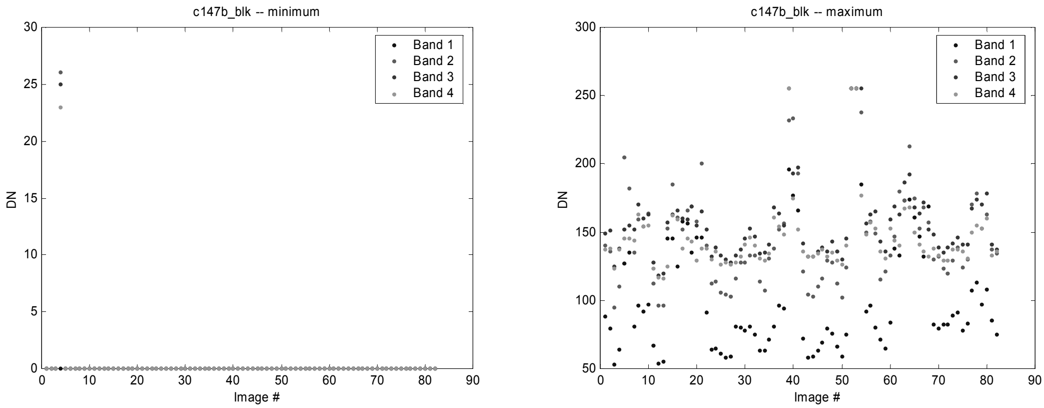

Figure 19. Minimum and maximum DN's in each band of every image in a data set.

Figure 20 shows that there are at most just a few saturated pixels in the images. Although the saturation somewhat coincides with the presence of the gray scale target in the images, close examination with the ENVI software showed that the saturation is caused by reflections from other objects than the gray panels and does not affect the radiometric tests. All the image statistics suggest that quality of images in this data set meets expectations.

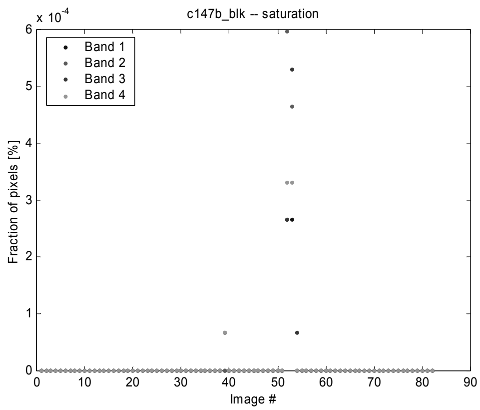

Figure 20. Portion of saturated pixels.

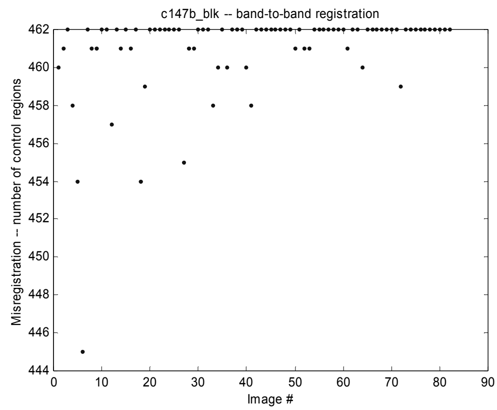

Figure 21. Number of regions selected in each image to evaluate spectral registration.

The number of regions selected in each image for evaluation of the spectral registration is shown in Figure 21. For all the images, the number of regions exceeds 400. It indicates that the program did not have problems with calculating the spectral registration in this data set. Mean misregistration is about 0.35 pixel with standard deviation of about 0.2 pixel, for all the images in the data set (see Figure 22).

Figure 23 shows that portion of regions misregistered by more than 0.5 pixel is approximately between 10% and 20%, while the portion of regions misregistered by more than one pixel is always smaller than 2%. Overall, in the entire data set, less than 0.4% of the tested regions are misregistered by more than 1 pixel.

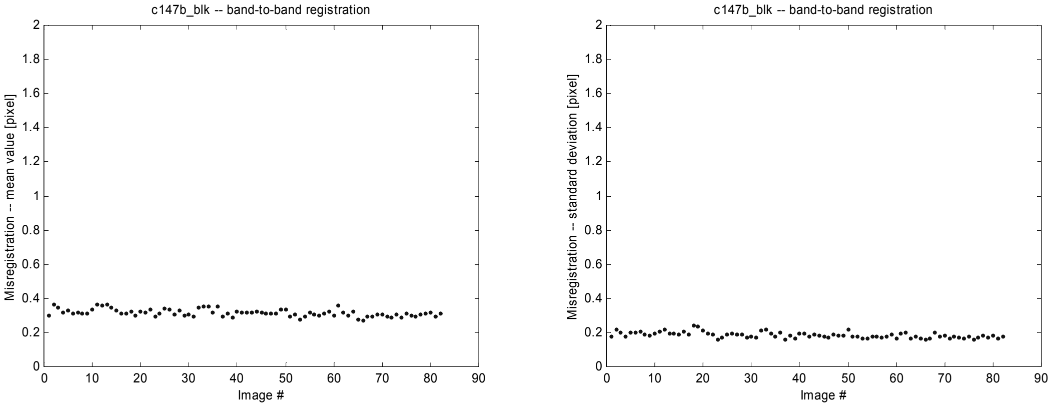

Figure 22. Mean and standard deviation of spectral misregistration.

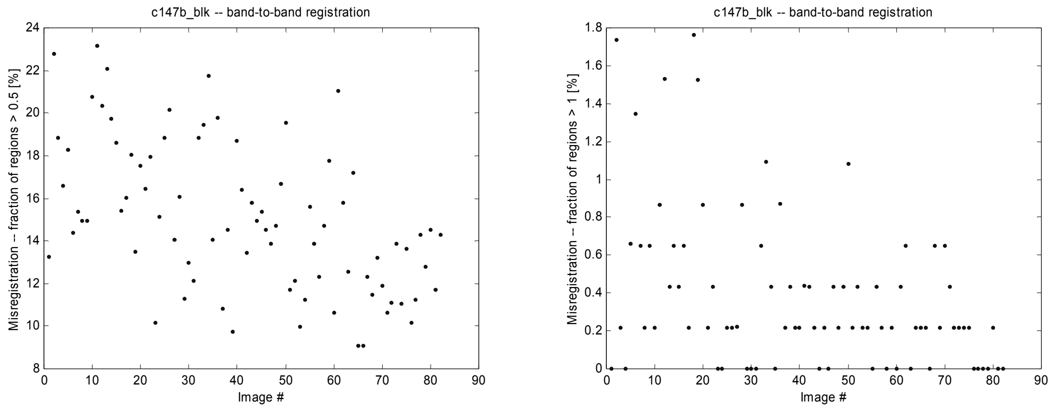

Figure 23. Portion of regions with spectral misregistration larger than 0.5 pixel (left) and one pixel (right).

Calculations of the image overlaps generated the results with the following statistical values:

```
75 endlaps
Mean endlap : 42.278194%
Std. dev.   : 2.464135%
Minimum     : 35.397453%
Maximum     : 45.769517%
Portion of endlaps smaller than 35% : 0.000000%

70 sidelaps
Mean sidelap : 43.056960%
Std. dev.    : 2.668369%
Minimum      : 38.276698%
Maximum      : 47.912062%
Portion of sidelaps smaller than 35% : 0.000000%
```

All the endlaps are in the range from 35% to 46%, and all the sidelaps are in the range from 38% to 48%. Therefore, all the overlaps are larger than the required 35%: they perfectly meet the requirements.

The calculated extent of the particular endlaps and sidelaps is listed below. The marks ">>" or "<>" at the beginning of each line mean that the images were acquired in the same or in the opposite direction, respectively.

```
Endlaps
>> c147b_blk_01_001 : c147b_blk_01_002 : 41.9185%
>> c147b_blk_01_002 : c147b_blk_01_003 : 41.5312%
>> c147b_blk_01_003 : c147b_blk_01_004 : 42.017%
>> c147b_blk_01_004 : c147b_blk_01_005 : 42.2324%
>> c147b_blk_01_005 : c147b_blk_01_006 : 42.2525%
>> c147b_blk_01_006 : c147b_blk_01_007 : 41.9001%
>> c147b_blk_01_007 : c147b_blk_01_008 : 41.7839%
>> c147b_blk_01_008 : c147b_blk_01_009 : 41.5763%
>> c147b_blk_01_009 : c147b_blk_01_010 : 42.177%
>> c147b_blk_01_010 : c147b_blk_01_011 : 42.0031%
>> c147b_blk_02_012 : c147b_blk_02_013 : 38.7246%
>> c147b_blk_02_013 : c147b_blk_02_014 : 39.4389%
>> c147b_blk_02_014 : c147b_blk_02_015 : 39.6682%
>> c147b_blk_02_015 : c147b_blk_02_016 : 39.4999%
>> c147b_blk_02_016 : c147b_blk_02_017 : 39.0169%
>> c147b_blk_02_017 : c147b_blk_02_018 : 37.961%
>> c147b_blk_02_018 : c147b_blk_02_019 : 38.2708%
>> c147b_blk_02_019 : c147b_blk_02_020 : 38.0717%
>> c147b_blk_02_020 : c147b_blk_02_021 : 37.8686%
>> c147b_blk_02_021 : c147b_blk_02_022 : 38.1171%
>> c147b_blk_03_023 : c147b_blk_03_024 : 43.1059%
>> c147b_blk_03_024 : c147b_blk_03_025 : 42.4066%
>> c147b_blk_03_025 : c147b_blk_03_026 : 42.1948%
>> c147b_blk_03_026 : c147b_blk_03_027 : 42.1117%
>> c147b_blk_03_027 : c147b_blk_03_028 : 42.0475%
>> c147b_blk_03_028 : c147b_blk_03_029 : 41.7727%
>> c147b_blk_03_029 : c147b_blk_03_030 : 42.2414%
>> c147b_blk_03_030 : c147b_blk_03_031 : 41.954%
>> c147b_blk_03_031 : c147b_blk_03_032 : 41.5252%
>> c147b_blk_03_032 : c147b_blk_03_033 : 41.5205%
>> c147b_blk_03_033 : c147b_blk_03_034 : 40.9372%
>> c147b_blk_04_035 : c147b_blk_04_036 : 45.2515%
>> c147b_blk_04_036 : c147b_blk_04_037 : 45.0603%
>> c147b_blk_04_037 : c147b_blk_04_038 : 45.041%
>> c147b_blk_04_038 : c147b_blk_04_039 : 45.4522%
```

```
>> c147b_blk_04_039 : c147b_blk_04_040 : 45.4301%
>> c147b_blk_04_040 : c147b_blk_04_041 : 45.1187%
>> c147b_blk_04_041 : c147b_blk_04_042 : 44.8028%
>> c147b_blk_04_042 : c147b_blk_04_043 : 44.2939%
>> c147b_blk_04_043 : c147b_blk_04_044 : 35.3975%
>> c147b_blk_04_044 : c147b_blk_04_045 : 43.0502%
>> c147b_blk_04_045 : c147b_blk_04_046 : 43.0196%
>> c147b_blk_05_047 : c147b_blk_05_048 : 42.1373%
>> c147b_blk_05_048 : c147b_blk_05_049 : 41.8637%
>> c147b_blk_05_049 : c147b_blk_05_050 : 41.2115%
>> c147b_blk_05_050 : c147b_blk_05_051 : 40.7031%
>> c147b_blk_05_051 : c147b_blk_05_052 : 40.6394%
>> c147b_blk_05_052 : c147b_blk_05_053 : 40.3825%
>> c147b_blk_05_053 : c147b_blk_05_054 : 39.9242%
>> c147b_blk_05_054 : c147b_blk_05_055 : 39.5422%
>> c147b_blk_05_055 : c147b_blk_05_056 : 39.2048%
>> c147b_blk_05_056 : c147b_blk_05_057 : 38.4738%
>> c147b_blk_05_057 : c147b_blk_05_058 : 37.8012%
>> c147b_blk_06_059 : c147b_blk_06_060 : 43.3605%
>> c147b_blk_06_060 : c147b_blk_06_061 : 44.0976%
>> c147b_blk_06_061 : c147b_blk_06_062 : 45.3657%
>> c147b_blk_06_062 : c147b_blk_06_063 : 45.7695%
>> c147b_blk_06_063 : c147b_blk_06_064 : 45.4515%
>> c147b_blk_06_064 : c147b_blk_06_065 : 45.2313%
>> c147b_blk_06_065 : c147b_blk_06_066 : 45.6102%
>> c147b_blk_06_066 : c147b_blk_06_067 : 44.9615%
>> c147b_blk_06_067 : c147b_blk_06_068 : 44.0193%
>> c147b_blk_06_068 : c147b_blk_06_069 : 43.5026%
>> c147b_blk_06_069 : c147b_blk_06_070 : 43.0087%
>> c147b_blk_07_071 : c147b_blk_07_072 : 42.1638%
>> c147b_blk_07_072 : c147b_blk_07_073 : 42.9481%
>> c147b_blk_07_073 : c147b_blk_07_074 : 44.2406%
>> c147b_blk_07_074 : c147b_blk_07_075 : 44.6376%
>> c147b_blk_07_075 : c147b_blk_07_076 : 44.8478%
>> c147b_blk_07_076 : c147b_blk_07_077 : 45.1167%
>> c147b_blk_07_077 : c147b_blk_07_078 : 44.7489%
>> c147b_blk_07_078 : c147b_blk_07_079 : 45.5187%
>> c147b_blk_07_079 : c147b_blk_07_080 : 45.3268%
>> c147b_blk_07_080 : c147b_blk_07_081 : 44.9679%
>> c147b_blk_07_081 : c147b_blk_07_082 : 44.3203%


Sidelaps
>< c147b_blk_01_001 : c147b_blk_02_022 : 47.632%
>< c147b_blk_01_002 : c147b_blk_02_022 : 47.215%
>< c147b_blk_01_003 : c147b_blk_02_021 : 46.7621%
>< c147b_blk_01_004 : c147b_blk_02_020 : 46.5398%
>< c147b_blk_01_005 : c147b_blk_02_019 : 46.5384%
>< c147b_blk_01_006 : c147b_blk_02_018 : 46.676%
>< c147b_blk_01_007 : c147b_blk_02_017 : 46.0042%
>< c147b_blk_01_008 : c147b_blk_02_016 : 44.1818%
>< c147b_blk_01_009 : c147b_blk_02_015 : 42.3052%
>< c147b_blk_01_010 : c147b_blk_02_014 : 41.1496%
>< c147b_blk_01_011 : c147b_blk_02_013 : 40.8897%
>< c147b_blk_02_012 : c147b_blk_03_034 : 39.0004%
>< c147b_blk_02_013 : c147b_blk_03_033 : 38.8713%
>< c147b_blk_02_014 : c147b_blk_03_032 : 39.7743%
>< c147b_blk_02_015 : c147b_blk_03_031 : 40.2214%
>< c147b_blk_02_016 : c147b_blk_03_030 : 40.7455%
>< c147b_blk_02_017 : c147b_blk_03_029 : 41.8939%
>< c147b_blk_02_018 : c147b_blk_03_028 : 43.1004%
>< c147b_blk_02_019 : c147b_blk_03_027 : 43.0807%
>< c147b_blk_02_020 : c147b_blk_03_026 : 42.5728%
>< c147b_blk_02_021 : c147b_blk_03_025 : 42.44%
>< c147b_blk_02_022 : c147b_blk_03_024 : 43.2286%
>< c147b_blk_03_023 : c147b_blk_04_046 : 46.398%
>< c147b_blk_03_024 : c147b_blk_04_046 : 46.7956%
>< c147b_blk_03_025 : c147b_blk_04_045 : 47.5893%
>< c147b_blk_03_026 : c147b_blk_04_044 : 47.9121%
>< c147b_blk_03_027 : c147b_blk_04_043 : 47.1959%
>< c147b_blk_03_028 : c147b_blk_04_042 : 45.6974%
>< c147b_blk_03_029 : c147b_blk_04_041 : 44.9477%
```

```
>< c147b_blk_03_030 : c147b_blk_04_040 : 44.7474%
>< c147b_blk_03_031 : c147b_blk_04_038 : 43.8045%
>< c147b_blk_03_032 : c147b_blk_04_037 : 44.1704%
>< c147b_blk_03_033 : c147b_blk_04_036 : 45.3886%
>< c147b_blk_03_034 : c147b_blk_04_035 : 45.5823%
>< c147b_blk_04_035 : c147b_blk_05_058 : 42.6954%
>< c147b_blk_04_036 : c147b_blk_05_057 : 42.4712%
>< c147b_blk_04_037 : c147b_blk_05_056 : 43.0655%
>< c147b_blk_04_038 : c147b_blk_05_055 : 43.637%
>< c147b_blk_04_039 : c147b_blk_05_055 : 43.6565%
>< c147b_blk_04_040 : c147b_blk_05_054 : 43.2055%
>< c147b_blk_04_041 : c147b_blk_05_053 : 42.372%
>< c147b_blk_04_042 : c147b_blk_05_052 : 41.3148%
>< c147b_blk_04_043 : c147b_blk_05_051 : 40.5478%
>< c147b_blk_04_044 : c147b_blk_05_050 : 40.0714%
>< c147b_blk_04_045 : c147b_blk_05_049 : 39.3262%
>< c147b_blk_04_046 : c147b_blk_05_048 : 38.3691%
>< c147b_blk_05_047 : c147b_blk_06_070 : 41.8428%
>< c147b_blk_05_048 : c147b_blk_06_069 : 41.0685%
>< c147b_blk_05_049 : c147b_blk_06_068 : 39.9459%
>< c147b_blk_05_050 : c147b_blk_06_067 : 40.1871%
>< c147b_blk_05_051 : c147b_blk_06_066 : 40.3192%
>< c147b_blk_05_052 : c147b_blk_06_065 : 40.1085%
>< c147b_blk_05_053 : c147b_blk_06_064 : 38.6513%
>< c147b_blk_05_054 : c147b_blk_06_063 : 38.2767%
>< c147b_blk_05_055 : c147b_blk_06_062 : 38.7231%
>< c147b_blk_05_056 : c147b_blk_06_061 : 39.9315%
>< c147b_blk_05_057 : c147b_blk_06_060 : 41.1773%
>< c147b_blk_05_058 : c147b_blk_06_059 : 42.4058%
>< c147b_blk_06_059 : c147b_blk_07_082 : 45.3231%
>< c147b_blk_06_060 : c147b_blk_07_081 : 44.9186%
>< c147b_blk_06_061 : c147b_blk_07_080 : 45.2521%
>< c147b_blk_06_062 : c147b_blk_07_079 : 46.039%
>< c147b_blk_06_063 : c147b_blk_07_078 : 46.0979%
>< c147b_blk_06_064 : c147b_blk_07_077 : 45.0246%
>< c147b_blk_06_065 : c147b_blk_07_076 : 43.502%
>< c147b_blk_06_066 : c147b_blk_07_075 : 42.3547%
>< c147b_blk_06_067 : c147b_blk_07_074 : 41.7012%
>< c147b_blk_06_068 : c147b_blk_07_073 : 42.2176%
>< c147b_blk_06_069 : c147b_blk_07_072 : 43.1648%
>< c147b_blk_06_070 : c147b_blk_07_071 : 43.9692%
```

References

CRSP-WI-21, *Product/Material Management*

CRSP-WI-22, *Verification of Commercial Data Shipments*

Freedman, E., *CRSP Radiometric Verification Recommendations*, Lockheed Martin Management and Data Systems, May 1999.

Lockheed Martin Space Operation – Stennis Programs (a), *Laboratory Characterization of Positive Systems ADAR 5500 Sensor: SN8 Linear*, Stennis Space Center, MS, August 1999.

Lockheed Martin Space Operations – Stennis Programs (b), *Validation of ADAR System 5500 Multispectral Mosaic*, Stennis Space Center, MS, *in preparation*.

MTL Systems, Inc., *Hopi I Gray Scale Deployment: Ground Truth Data Collection Report*, ITF-437-001, July 1999.

Shingoitewa-Honanie, G. and Jenner, J., *Full-Field-of-View Geodetic Target Range* in: Proceedings of the NASA Commercial Remote Sensing Verification and Validation Symposium, Stennis Space Center, MS, August 4-6, 1998.

Tzannes, A.P. and Mooney, J.M., *Optical Engineering*, Vol. 34, No.6, pp. 1808-1817, 1995.

Appendix A

FLIGHT LOG
(6-30-99)

- Customer name:	NASA - SDB
- Customer number:	c147
- Task Order:	Task Order #1
- Task Request:	Task Request - Test Flight
- Flight Crew:	Willie & Brad
- Data set:	a
- Site Name:	Winslow, AZ
- ADAR System:	SN-8
- Camera orientation:	1 & 2 Inverted
- Flight Altitude:	9,100, 11,700, 14,900, 18,100'MSL
- Ground elevation:	5,300'
- Wheels up at:	11:20 MDT
- Weather forecast:	Sunny
- Sky conditions on site:	Sunny
- On station at:	12:00 MDT

EXPOSURES:

Band 1	ISO=200, f 2.8,	shutter speed= 1250
Band 2	ISO=200, f 2.8,	shutter speed= 2500
Band 3	ISO=200, f 4.0,	shutter speed= 800
Band 4	ISO=200, f 5.6,	shutter speed= 800

NOTE: Data is very dark in bands 1 & 2 due to the fact that we could not have any saturation of the radiometric panels.

LINE#	HEADING	IMAGE#'s	NOTES
grnd_dark	n/a	001-010	Dark imgs on the ground. Temp 34.8C.
.75_1dark	n/a	013-023	1st dark at .75mpp. Temp 22.7C.
Single Lines: .75mpp			
.75_01	083	122-131	
.75_02	353	132-142	
.75_03	083	143-152	
.75_04	353	153-163	
.75_05	083	164-172	
.75_06	353	173-183	
.75_2dark	n/a	184-193	2nd dark at .75mpp. Temp 16.9C.
Single Lines: 1mpp			
1_1dark	n/a	194-203	1st dark at 1mpp. Temp 16.4C.
1_01	353	204-210	
1_02	083	211-217	
1_03	353	218-224	
1_04	083	225-231	
1_05	353	232-238	
1_06	083	239-245	
1_2dark	n/a	246-255	2nd dark at 1mpp. Temp 19.3C.

Single Lines: .5mpp

.5_1dark	n/a	256-265	1st dark at .5mpp. Temp 20.7C.
.5_01	083	266-276	
.5_02	353	277-289	
.5_03	083	290-301	
.5_04	353	302-314	
.5_05	083	315-326	
.5_06	353	327-338	
.5_2dark	n/a	339-348	2nd dark at .5mpp. Temp 25.0C.

Single Lines: .3mpp

.3_1dark	n/a	349-369	1st dark at .3mpp. Temp 27.2C.
.3_01	353	370-382	rough flight at 0.3mpp.
.3_02	083	383-393	
.3_03	353	413-420	reflight of line 03.
.3_04	083	421-428	
.3_05	353	429-439	
.3_06	083	440-447	
.3_2dark	n/a	448-455	2nd dark at .3mpp. Temp 31.1C.

Last image: 15:30 MDT

Appendix B

FLIGHT LOG
(7-1-99)

- Customer name:	NASA
- Customer number:	c147
- Task Order:	Task Order #1
- Task Request:	Task Request - Test Flight
- Flight Crew:	Willie & Brad
- Data set:	b
- Site Name:	Winslow, AZ
- ADAR System:	SN-8
- Camera orientation:	1,2 inverted
- Flight Altitude:	14,900ft MSL
- Ground elevation:	5,300ft
- Wheels up at:	10:30 MDT
- Weather forecast:	Sunny
- Sky conditions on site:	Sunny
- On station at:	11:00 MDT

EXPOSURES:

Band 1	ISO=200,	f 2.8,	shutter speed= 1250
Band 2	ISO=200,	f 2.8,	shutter speed= 2500
Band 3	ISO=200,	f 4.0,	shutter speed= 800
Band 4	ISO=200,	f 5.6,	shutter speed= 800

LINE#	HEADING	IMAGE#'s	NOTES
blk_01	090	01-11	
blk_02	270	12-22	
blk_03	090	23-34	
blk_04	270	35-46	
blk_05	090	47-58	
blk_06	270	59-70	
blk_07	090	71-82	

Last Image: 11:30 MDT

Customer Data Sheet

RE: c147 – Delivery Task Order #1; Task Request – Test Flight; Site: Winslow, AZ

I. Image Format

A. Images are in ERDAS ".lan" format

B. This delivery includes images captured in two datasets:

c147	flight day 1
c147b	flight day 2

C. File naming convention:

c147*_xx_??_###r.lan

c147	project ID
*	dataset distinction (b for block site)
xx	imagery descriptor (.3, .5, .75, 1, dark, blk)
??	flight line
###	scene number
r	indicates that the image has been spectrally co-registered (not present for dark images)
.lan	ERDAS .lan extension

Dataset	Images	# of Images
flight day 1	0.3 mpp GSD	59
	0.5 mpp GSD	73
	0.75 mpp GSD	62
	1 mpp GSD	42
	dark images	103
flight day 2 (b)	block site	82

D. Number of images delivered: 421

E. Data volume: 2.52 GB

II. Flight Line Layout

A. Average Spatial Resolutions: 0.3, 0.5, 0.75, and 1 meter/pixel GSD

B. Desired Overlap: 35% end and 35% side for block site

C. Aircraft Altitude:

0.3 mpp	9,100' MSL
0.5 mpp	11,700' MSL
0.75 mpp	14,900' MSL
1 mpp	18,100' MSL
block site	14,900' MSL
dark images	acquired at 9,100', 11,700', 14,900', and 18,100' MSL

D. Average Image Footprint Size:

300 x 450 meters @ 0.3 meter/pixel GSD
500 x 750 meters @ 0.5 meter/pixel GSD
750 x 1125 meters @ 0.75 meter/pixel GSD
1000 x 1500 meters @ 1 meter/pixel GSD

E. Desired Heading:

1. Individual tarp flights at resolutions of 0.3mpp, 0.5mpp, 0.75mpp, and 1mpp GSD:

Flight Line	Heading (degrees N)
01	83
02	353
03	83
04	353
05	83
06	353

2. Block site:

Flight Line	Heading (degrees N)
01	90
02	270
03	90
04	270
05	90
06	270
07	90

3. Dark images: heading varies – not applicable.

F. Number of Flight Lines:

1. Tarp flights: 6 flight lines at each resolution
2. Block site: 7 flight lines
3. Dark images: 2 flight lines at each resolution

G. Flight log information:

For flight log information, please refer to the individual flight logs included with this delivery. There are two flight logs, provided in both hardcopy and electronic format, one for each dataset (each day of image acquisition). The flight log names are:

c147_flt_log.txt flight day 1
c147b_flt_log.txt flight day 2

III. Sensor Information – Sensor used for this project was SN8

A. Spectral Bands and Band Widths

Band	Bandwidth (nm)	Color
1	450-515	Blue
2	525-605	Green
3	630-690	Red
4	750-900	Near IR

B. Location of sensors in the housing:
(direction of flight towards top of page)

1	2
4	3

The two forward sensors, in this case #1 and #2, record images which are inverted compared to images captured by the other two sensors, #3 and #4.

IV. Dark Image Information

Image Name Prefixes	Resolution	06/30/99 Approximate Time (GMT)	Temperature (°C)
c147_.3_1dark	0.3 mpp	21:48	27.2
c147_.3_2dark	0.3 mpp	22:27	31.1
c147_.5_1dark	0.5 mpp	21:10	20.7
c147_.5_2dark	0.5 mpp	21:42	25.0
c147_.75_1dark	0.75 mpp	18:47	22.7
c147_.75_2dark	0.75 mpp	20:17	16.9
c147_1_1dark	1 mpp	20:28	16.4
c147_1_2dark	1 mpp	20:58	19.3
c147_grnd_dark	N/A	18:05	34.8

V. GPS Information

The GPS files are in electronic format on the enclosed CD-ROM and on the 8mm image delivery tape:

c147_.3_gps.txt
c147_.5_gps.txt
c147_.75_gps.txt
c147_1_gps.txt
c147_dark_gps.txt
c147b_block_gps.txt

The GPS text file includes one world geodetic coordinate for each image captured. These latitude/longitude coordinates are generated utilizing the NAD 27 datum to reflect the approximate camera exposure station for each image. These files include scene number, dataset, direction of flight, exact time of image capture, approximate latitude/longitude, and elevation of the aircraft at the time of image capture. See the enclosed GPS technical note for a description of the GPS text data, provided in both hardcopy and electronic format. The electronic file on the CD-ROM is named *gps_tech.txt*.

VI. Post Processing

A. Fully Processed Images (individual tarp images and block site):

1. All fully processed images are on the enclosed 8mm tape.
2. All fully processed images are in ERDAS ".lan" format.
3. Bands 1 & 2 have been rotated 180 degrees to match bands 3 & 4.
4. Images have been corrected for sensor nonuniformities.
5. Images have been corrected for lens vignetting effects.
6. Images have had a dark sample subtraction value of 8 applied.
7. Images have been spectrally co-registered using the nearest neighbor algorithm.

B. Dark Images:

1. All dark images are on the enclosed 8mm tape.
2. All dark images are in ERDAS ".lan" format.
3. For all dark images, bands 1 & 2 have **not** been rotated 180 degrees to match bands 3 & 4.
4. No post-processing has been performed on the dark images (i.e., no correction for sensor nonuniformities, no correction for lens vignetting effects, no dark sample subtraction, and no spectral co-registration).

VII. Processing Notes

A. The reflectance panels may be found in the following images:

0.3 mpp	0.5 mpp	0.75 mpp	1 mpp
*c147_.3_01_376r.lan	c147_.5_01_271r.lan	c147_.75_01_127r.lan	c147_1_01_206r.lan
c147_.3_02_389r.lan	c147_.5_01_272r.lan	c147_.75_01_128r.lan	c147_1_02_214r.lan
c147_.3_03_417r.lan	c147_.5_02_282r.lan	c147_.75_02_137r.lan	c147_1_02_215r.lan
*c147_.3_04_426r.lan	c147_.5_02_283r.lan	c147_.75_03_147r.lan	c147_1_03_221r.lan
c147_.3_05_436r.lan	c147_.5_03_296r.lan	c147_.75_03_148r.lan	c147_1_04_228r.lan
c147_.3_06_445r.lan	c147_.5_04_307r.lan	c147_.75_04_157r.lan	c147_1_05_235r.lan
	c147_.5_04_308r.lan	c147_.75_04_158r.lan	c147_1_06_242r.lan
	c147_.5_05_320r.lan	c147_.75_05_168r.lan	c147_1_06_243r.lan
	c147_.5_06_332r.lan	c147_.75_05_169r.lan	
		c147_.75_06_178r.lan	

* Portions of the panels were cut off in these images due to turbulent flight conditions in the 0.3 mpp imagery.

B. A slight blurring effect was noticed on the imagery, possibly caused by a film of oil from airplane exhaust on the camera lenses.

C. The imagery is dark due to the requirement that the reflectance panels could not have any saturation.

D. The enclosed metadata is not in ECS metadata format. That reformatted data will be provided in a later delivery.

VIII. Enclosures

A. The enclosed CD-ROM contains electronic copies of the following metadata:

1. Delivery Cover Letter
   c147-NASA-SDB-AZ_Task1_ReqTestFlight_Delivery_Letter.doc
2. Customer Data Sheet
   c147-NASA-SDB-AZ_Task1_ReqTestFlight_Data_Sheet.doc
3. Flight Logs (2 files)
   c147_flt_log.txt
   c147b_flt_log.txt
4. GPS text files
   c147_.3_gps.txt
   c147_.5_gps.txt
   c147_.75_gps.txt
   c147_1_gps.txt
   c147_dark_gps.txt
   c147b_block_gps.txt
5. "Include" file containing a list of files included on the delivery tape
   c147_delv_incl
6. Instrument Specifications
   ADAR5500_spec (PageMaker document)
7. GPS Technical Note
   gps_tech.txt

B. The enclosed 8mm data tape contains 421 images. Total data volume is 2.52 GB.

C. Hardcopies of the following files are provided:

1. Frame index maps are provided in several layouts and sections for ease of viewing. These maps indicate the approximate location of each image over the site. The

frame index is a graphical representation of the image coverage, derived from the GPS text files.

2. Flight logs are provided about specific flight and image acquisition information for each day of image capture.

3. The image delivery tape “include” file is provided that lists the filenames included on the 8mm tape.

4. ADAR 5500 Instrument Specification sheet.

5. GPS Technical Note.

Appendix D

Image file index used on the horizontal axes of the graphs created during validation of image products:

```
1: c147b_blk_01_001r.lan
2: c147b_blk_01_002r.lan
3: c147b_blk_01_003r.lan
4: c147b_blk_01_004r.lan
5: c147b_blk_01_005r.lan
6: c147b_blk_01_006r.lan
7: c147b_blk_01_007r.lan
8: c147b_blk_01_008r.lan
9: c147b_blk_01_009r.lan
10: c147b_blk_01_010r.lan
11: c147b_blk_01_011r.lan
12: c147b_blk_02_012r.lan
13: c147b_blk_02_013r.lan
14: c147b_blk_02_014r.lan
15: c147b_blk_02_015r.lan
16: c147b_blk_02_016r.lan
17: c147b_blk_02_017r.lan
18: c147b_blk_02_018r.lan
19: c147b_blk_02_019r.lan
20: c147b_blk_02_020r.lan
21: c147b_blk_02_021r.lan
22: c147b_blk_02_022r.lan
23: c147b_blk_03_023r.lan
24: c147b_blk_03_024r.lan
25: c147b_blk_03_025r.lan
26: c147b_blk_03_026r.lan
27: c147b_blk_03_027r.lan
28: c147b_blk_03_028r.lan
29: c147b_blk_03_029r.lan
30: c147b_blk_03_030r.lan
31: c147b_blk_03_031r.lan
32: c147b_blk_03_032r.lan
33: c147b_blk_03_033r.lan
34: c147b_blk_03_034r.lan
35: c147b_blk_04_035r.lan
36: c147b_blk_04_036r.lan
37: c147b_blk_04_037r.lan
38: c147b_blk_04_038r.lan
39: c147b_blk_04_039r.lan
40: c147b_blk_04_040r.lan
41: c147b_blk_04_041r.lan
42: c147b_blk_04_042r.lan
43: c147b_blk_04_043r.lan
44: c147b_blk_04_044r.lan
45: c147b_blk_04_045r.lan
46: c147b_blk_04_046r.lan
47: c147b_blk_05_047r.lan
48: c147b_blk_05_048r.lan
49: c147b_blk_05_049r.lan
50: c147b_blk_05_050r.lan
51: c147b_blk_05_051r.lan
52: c147b_blk_05_052r.lan
53: c147b_blk_05_053r.lan
54: c147b_blk_05_054r.lan
55: c147b_blk_05_055r.lan
56: c147b_blk_05_056r.lan
57: c147b_blk_05_057r.lan
58: c147b_blk_05_058r.lan
59: c147b_blk_06_059r.lan
60: c147b_blk_06_060r.lan
61: c147b_blk_06_061r.lan
62: c147b_blk_06_062r.lan
63: c147b_blk_06_063r.lan
64: c147b_blk_06_064r.lan
65: c147b_blk_06_065r.lan
66: c147b_blk_06_066r.lan
67: c147b_blk_06_067r.lan
68: c147b_blk_06_068r.lan
69: c147b_blk_06_069r.lan
70: c147b_blk_06_070r.lan
71: c147b_blk_07_071r.lan
72: c147b_blk_07_072r.lan
73: c147b_blk_07_073r.lan
74: c147b_blk_07_074r.lan
75: c147b_blk_07_075r.lan
76: c147b_blk_07_076r.lan
77: c147b_blk_07_077r.lan
78: c147b_blk_07_078r.lan
79: c147b_blk_07_079r.lan
80: c147b_blk_07_080r.lan
81: c147b_blk_07_081r.lan
82: c147b_blk_07_082r.lan
```

Appendix E

MATLAB function that calculates image statistics and spectral registration for a set of images:

```
function [] = calc_PosSys( dirname )
% Performs calculations for validation of a set of Positive Systems' ADAR 5500 imagery

% Set data set identification name by extracting the current subdirectory name from the full
directory name

delimiter = fullfile( '1', '3' ); delimiter = delimiter(2); % find separator
k = findstr( dirname, delimiter ); k = max( k );            % find position of the last separator
ident = dirname(k + 1:end);                                 % extract the last subdirectory

% Select image file format (set for ADAR 5500 imagery)

filetype = 'LAN';
file_ext = lower( filetype );

% Get list of files

filelist = dir( fullfile( dirname, [ '*.' file_ext ] ) );
nframes = size( filelist, 1 );

% Print the image file names into the index file

filename = fullfile( dirname, [ 'index_' ident '.txt' ] );
fid = fopen( filename, 'wt' );
for id = 1 : nframes
  fprintf( fid, '%d : %s\n', id, filelist(id).name );
end
fclose( fid );

% Get image specifications from the first file

filename = fullfile( dirname, filelist(1).name );
image_cube = open_image_cube_file( filename, filetype );
close_image_cube_file( image_cube )

% Set parameter for calculations of statistics

sat_level = 2 ^ ( 8 * image_cube.nbytes ) - 1;  % maximum DN (saturation level)

% Set parameters for calculations of spectral registration

n = 17; % cross-correlation block size
m = 8;  % peak block size
k = 16; % resolution enhancement factor

overlaps = 0.35;  % frame overlaps
skip = 5;         % no. of control regions to skip

% Initialize matrices for statistics

avg_frame = zeros( nframes, image_cube.nbands );
std_frame = zeros( nframes, image_cube.nbands );
skw_frame = zeros( nframes, image_cube.nbands );
kur_frame = zeros( nframes, image_cube.nbands );
min_frame = zeros( nframes, image_cube.nbands );
max_frame = zeros( nframes, image_cube.nbands );
sat_frame = zeros( nframes, image_cube.nbands );

% Initialize matrices for spectral registration

avg_misreg = zeros( nframes, 1 );
std_misreg = zeros( nframes, 1 );
len_misreg = zeros( nframes, 1 );
num_misreg = zeros( nframes, 1 );
one_misreg = zeros( nframes, 1 );
```

```
% Initialize matrix for band correlation

corr_band = zeros( nframes, image_cube.nbands * ( image_cube.nbands - 1 ) / 2 );

% Calculate statistics for each image

for iframe = 1 : nframes

  % read image file from disk
  filename = fullfile( dirname, filelist(iframe).name );
  image_cube = open_image_cube_file( filename, filetype );
  image_cube.data = read_image_cube_tile( image_cube, [] );
  close_image_cube_file( image_cube )

  % calculate statistics for each band
  for iband = 1 : image_cube.nbands
    frame = double( image_cube.data(:,:,iband) );
    frame = frame(:);
    avg_frame(iframe,iband) = mean( frame );
    std_frame(iframe,iband) = std( frame );
    skw_frame(iframe,iband) = skewness( frame );
    kur_frame(iframe,iband) = kurtosis( frame );
    min_frame(iframe,iband) = min( frame );
    max_frame(iframe,iband) = max( frame );
    sat_frame(iframe,iband) = sum( frame == sat_level ) / length( frame );
  end

  % calculate misregistration between all the bands
  nbrows = floor( ( 1 - overlaps ) * image_cube.nrows / ( skip * n ) );
  nbcols = floor( ( 1 - overlaps ) * image_cube.ncols / ( skip * n ) );
  row0 = floor( ( image_cube.nrows - skip * n * nbrows ) / 2 );
  col0 = floor( ( image_cube.ncols - skip * n * nbcols ) / 2 );
  misreg = zeros( nbrows, nbcols, image_cube.nbands * ( image_cube.nbands - 1 ) / 2 );
  frame = [];
  for ib = 1 : nbrows
    rows = [ 1 : n ] + row0 + ( ib - 1 ) * skip * n;
    for jb = 1 : nbcols
      cols = [ 1 : n ] + col0 + ( jb - 1 ) * skip * n;
      for iband = 1 : image_cube.nbands
        frame(:,:,iband) = double( image_cube.data(rows,cols,iband) );
        frame(:,:,iband) = frame(:,:,iband) - mean2( frame(:,:,iband) );
      end
      ipair = 0;
      for iband = 1 : image_cube.nbands - 1
        for jband = iband + 1 : image_cube.nbands
          xc = xcorr2( frame(:,:,iband), frame(:,:,jband) );
          xc = xc(1 : end - 1,1 : end - 1);
          xc = xc(( end - m ) / 2 + 1 : ( end + m ) / 2,( end - m ) / 2 + 1 : ( end + m ) / 2);
          % enhance spatial resolution
          u = fftshift( fft2( xc ) );
          v = cat( 1, zeros( ( k - 1 ) * size( u, 1 ) / 2, size( u, 2 ) ), u, ...
                      zeros( ( k - 1 ) * size( u, 1 ) / 2, size( u, 2 ) ) );
          v = cat( 2, zeros( size( v, 1 ), ( k - 1 ) * size( u, 2 ) / 2 ), v, ...
                      zeros( size( v, 1 ), ( k - 1 ) * size( u, 2 ) / 2 ) );
          yc = abs( ifft2( v ) );
          % estimate misregistration
          [ i, j ] = find( yc == max( yc(:) ) );
          dist = sqrt( ( k * m / 2 + 1 - i(1) )^2 + ( k * m / 2 + 1 - j(1) )^2 ) / k;
          ipair = ipair + 1;
          misreg(ib,jb,ipair) = dist;
        end
      end
    end
  end
  misreg = misreg(find( misreg < 2 ));
  avg_misreg(iframe) = mean( misreg(:) );
  std_misreg(iframe) = std( misreg(:) );
  len_misreg(iframe) = length( misreg(:) );
  num_misreg(iframe) = sum( misreg(:) > 0.5 ) / len_misreg(iframe);
  one_misreg(iframe) = sum( misreg(:) > 1 ) / len_misreg(iframe);
```

```
  % calculate correlation between bands
  ipair = 0;
  for iband = 1 : image_cube.nbands - 1
    for jband = iband + 1 : image_cube.nbands
      ipair = ipair + 1;
      corr_band(iframe,ipair) = corr2( image_cube.data(:,:,iband), image_cube.data(:,:,jband) );
    end
  end

end

% Save results

filename = fullfile( dirname, [ 'matrix_' ident '.mat' ] );
save( filename, 'dirname', ...
      'avg_frame', 'std_frame', 'skw_frame', 'kur_frame', 'min_frame', 'max_frame', 'sat_frame',
...
      'avg_misreg', 'std_misreg', 'num_misreg', 'len_misreg', 'one_misreg', ...
      'corr_band' )

return
```

Appendix F

MATLAB function that calculates image overlaps for a set of ADAR 5500 images.

```
function [] = frame_overlaps( dirname, gpsfile, demdir )
% Uses a Postitive Systems GPS output file and scene information
% to extract georeference data (location, time, heading, image size)
% and calculate endlaps and sidelaps between images

% Set data set identification name by extracting the current subdirectory name from the full
directory name

delimiter = fullfile( '1', '3' ); delimiter = delimiter(2); % find separator
k = findstr( dirname, delimiter ); k = max( k );            % find position of the last separator
ident = dirname(k + 1:end);                                 % extract the last subdirectory

% Select image file format (set for ADAR 5500 imagery)

filetype = 'LAN';
file_ext = lower( filetype );

% Set some constants (these would be passed in if a GUI were used)

ft2km = 12 * 25.4 * 1e-6; % km/ft = in/ft * mm/in * km/mm
radius = 6378.137;        % earth radius [km]

end_spec = 0.35;  % endlap requirement
side_spec = 0.35; % sidelap requirement

ifov_x = 0.257e-3; % ADAR 5500 cross-track IFOV (sampling interval) [rad]
ifov_l = 0.257e-3; % ADAR 5500 along-track IFOV (sampling interval) [rad]

% Read in the GPS file and get the Dataset #,
% Latitude, Longitude, Altitude, and Heading.

iframe = 0;
nlines = 0;
dataset = [];
flight_line = [];
fid = fopen( fullfile( dirname, gpsfile ) , 'r' );
while ~feof( fid )
  line = fgetl( fid );
  if isempty( line ); break; end; % there may be two empty lines at the end of the file
  iframe = iframe + 1;
   dataset = strvcat( dataset, sscanf ( line, '%*s %s', 1 ) );
  % detect a new flight line and note its name to the list of the flight lines
  % (assuming that all the images from one flight line are listed together in the GPS file)
  if ( iframe == 1 ) | ~strcmp( dataset(iframe,:), dataset(iframe - 1,:) )
    nlines = nlines + 1;
    flight_line = strvcat( flight_line, dataset(iframe,:) );
  end
  % get scene (image) number
  line = fgetl( fid );
   scene_num(iframe) = sscanf( line, '%*s %*s %d', 1 );
  % check order of images in the same flight line
  if ( iframe > 1 ) & strcmp( dataset(iframe,:), dataset(iframe - 1,:) ) & ...
      ( scene_num(iframe) <= scene_num(iframe - 1) )
    disp( [ 'Warning: image ' deblank( dataset(iframe,:) ) sprintf( '_%03u', scene_num(iframe) )
...
             ' follows ' deblank( dataset(iframe - 1,:) ) sprintf( '_%03u', scene_num(iframe - 1)
) ] )
  end
  line = fgetl( fid );
   latitude(iframe) = sscanf( line, '%*s %f', 1 );
   hemisphere = sscanf( line, '%*s %*f %*s %s', 1 );
  if strcmp( hemisphere, 'S' )
    latitude(iframe) = - latitude(iframe);
  end
   longitude(iframe) = sscanf( line, '%*s %*f %*s %*s %*s %f', 1);
   direction = sscanf( line, '%*s %*f %*s %*s %*s %*f %*s %s', 1);
```

```
  if strcmp( direction, 'W' )
    longitude(iframe) = - longitude(iframe);
  end
  line = fgetl( fid );
   altitude(iframe) = sscanf( line, '%*s %f', 1);
  line = fgetl( fid );
   heading(iframe) = sscanf( line, '%*s %f', 1);
  line = fgetl( fid );
  line = fgetl( fid );
  % get the frame size from the image file header
  filename = [ deblank( dataset(iframe,:) ) sprintf( '_%03u', scene_num(iframe) ) 'r.' file_ext
];
  image_cube = read_LAN_header( fullfile( dirname, filename ) );
  scene_rows(iframe) = image_cube.nrows;
  scene_cols(iframe) = image_cube.ncols;
  % find ground elevation from the DEM data
  [ filename, quadrangle ] = usgsdems( latitude(iframe), longitude(iframe) );
  filename = char( filename{1} ); % convert cell to string
  [ dem, leg ] = usgsdem( fullfile( demdir, filename ), 1, ...
                        [ latitude(iframe) latitude(iframe) ], [ longitude(iframe)
longitude(iframe) ] );
  elevation(iframe) = dem(1,1) * 1e-3;  % [m] -> [km]
end
fclose( fid );
nframes = iframe;

% Define adjacent flight lines

adjacent_flight_line = [];
filename = 'adjacent_flight_lines.txt';
if exist( fullfile( dirname, filename ) ) == 2
  % overwrite default line order using data in the file
  fid = fopen( fullfile( dirname, filename ) , 'r' );
  while ~feof( fid )
    line = fgetl( fid );
    adjacent_flight_line = strvcat( adjacent_flight_line, line );
  end
  fclose( fid );
else
  % create the default list: the adjacent flight line is the next one
  for i = 1 : nlines - 1
    adjacent_flight_line = strvcat( adjacent_flight_line, [ flight_line(i,:) ' ' flight_line(i +
1,:) ] );
  end
end
%
for i = 1 : nframes
  j = strmatch( [ deblank( dataset(i,:) ) ' ' ], adjacent_flight_line );
  if isempty( j )
    line_id(i) = 0;
  else
    line_id(i) = j;
  end
end

% Get half of image size [km]

alongtrack = tan( ifov_l * scene_rows / 2 ) .* ( altitude * ft2km - elevation );
crosstrack = tan( ifov_x * scene_cols / 2 ) .* ( altitude * ft2km - elevation );

% Change azimuth to trigonometric angle

angle = 90 - heading + 360 * ( heading >= 270 );

% Change degrees to radians

latitude = latitude * pi / 180;
longitude = longitude * pi / 180;
angle = angle * pi / 180;

% Calculate image versors
```

```
vx = cos( angle );
vy = sin( angle );

% Open the output file

filename = fullfile( dirname, [ 'endlaps_sidelaps_' ident '.txt' ] );
fid = fopen( filename, 'wt' );

% Calculate endlaps (within each flight line)

fprintf( fid, 'Endlaps\n' );

count = 0;
for i = 1 : nframes - 1
  j = i + 1;
  % ensures that only frames in the same flight line are compared
  if strcmp( dataset(i,:), dataset(j,:) )
    count = count + 1;
    % project distance and sizes onto the direction of mean azimuth
    if ( vx(i) * vx(j) + vy(i) * vy(j) ) > 0
      % flight lines in the same direction
      endlap(count) = 1 - radius * ...
                          abs( ( vx(i) + vx(j) ) * ( longitude(j) - longitude(i) ) * ...
                                                   cos( ( latitude(i) + latitude(j) ) / 2 ) + ...
                               ( vy(i) + vy(j) ) * ( latitude(j) - latitude(i) ) ) / ...
                          abs( ( vx(i) + vx(j) ) * ( alongtrack(i) * vx(i) + alongtrack(j) *
vx(j) ) + ...
                               ( vy(i) + vy(j) ) * ( alongtrack(i) * vy(i) + alongtrack(j) *
vy(j) ) );
      line = [ '>> ' deblank( dataset(i,:) ) sprintf( '_%03u', scene_num(i) ) ' : ' ...
                     deblank( dataset(j,:) ) sprintf( '_%03u', scene_num(j) ) ' : ' ...
                 num2str( 100 * endlap(count) ) '%' ];
    else
      % flight lines in the opposite directions
      endlap(count) = 1 - radius * ...
                          abs( ( vx(i) - vx(j) ) * ( longitude(j) - longitude(i) ) * ...
                                                   cos( ( latitude(i) + latitude(j) ) / 2 ) + ...
                               ( vy(i) - vy(j) ) * ( latitude(j) - latitude(i) ) ) / ...
                          abs( ( vx(i) - vx(j) ) * ( alongtrack(i) * vx(i) - alongtrack(j) *
vx(j) ) + ...
                               ( vy(i) - vy(j) ) * ( alongtrack(i) * vy(i) - alongtrack(j) *
vy(j) ) );
      line = [ '>< ' deblank( dataset(i,:) ) sprintf( '_%03u', scene_num(i) ) ' : ' ...
                     deblank( dataset(j,:) ) sprintf( '_%03u', scene_num(j) ) ' : ' ...
                 num2str( 100 * endlap(count) ) '%' ];
    end
    if endlap(count) > 0
      fprintf( fid, '%s\n', line );
    else
      fprintf( fid, '%s !!! GAP !!!\n', line );
    end
  end
end

% Calculate sidelaps (between flight lines)

fprintf( fid, '\nSidelaps\n' );

count = 0;
for i = 1 : nframes - 1
  % find the closest image from the adjacent flight line
  dist_min = Inf;
  for j = i + 1 : nframes
    % not the last line & not the same line & it is the adjacent line
    if ( line_id(i) > 0 ) & ~strcmp( dataset(i,:), dataset(j,:) ) & ...
       ~isempty( findstr( deblank( dataset(j,:) ), adjacent_flight_line(line_id(i),:) ) )
      % calculate distance between image centers
      dx = ( longitude(j) - longitude(i) ) * cos( ( latitude(i) + latitude(j) ) / 2 );
      dy = ( latitude(j) - latitude(i) );
      dd = radius * sqrt( dx * dx + dy * dy );
```

```
      if dd < dist_min
        dist_min = dd;
        j_min = j;
      end
    end
  end
  % if the image exists
  if dist_min < Inf
    j = j_min;
    if ( vx(i) * vx(j) + vy(i) * vy(j) ) > 0
      % flight lines in the same direction
      % estimate apparent endlap
      endlap_ = 1 - radius * ...
                  abs( ( vx(i) + vx(j) ) * ( longitude(j) - longitude(i) ) * ...
                                         cos( ( latitude(i) + latitude(j) ) / 2 ) + ...
                       ( vy(i) + vy(j) ) * ( latitude(j) - latitude(i) ) ) / ...
                  abs( ( vx(i) + vx(j) ) * ( alongtrack(i) * vx(i) + alongtrack(j) * vx(j) ) +
...
                       ( vy(i) + vy(j) ) * ( alongtrack(i) * vy(i) + alongtrack(j) * vy(j) ) );
      if endlap_ > 0
        % include sidelap only when the endlap exists
        count = count + 1;
        sidelap(count) = 1 - radius * ...
                         abs( ( vy(i) + vy(j) ) * ( longitude(j) - longitude(i) ) * ...
                                                cos( ( latitude(i) + latitude(j) ) / 2 ) -
...
                              ( vx(i) + vx(j) ) * ( latitude(j) - latitude(i) ) ) / ...
                         abs( ( vx(i) + vx(j) ) * ( crosstrack(i) * vx(i) + crosstrack(j) *
vx(j) ) + ...
                              ( vy(i) + vy(j) ) * ( crosstrack(i) * vy(i) + crosstrack(j) *
vy(j) ) );
        line = [ '>> ' deblank( dataset(i,:) ) sprintf( '_%03u', scene_num(i) ) ' : ' ...
                       deblank( dataset(j,:) ) sprintf( '_%03u', scene_num(j) ) ' : ' ...
                 num2str( 100 * sidelap(count) ) '%' ];
        if sidelap(count) > 0
          fprintf( fid, '%s\n', line );
        else
          fprintf( fid, '%s !!! GAP !!!\n', line );
        end
      end
    else
      % flight lines in the opposite directions
      % estimate apparent endlap
      endlap_ = 1 - radius * ...
                  abs( ( vx(i) - vx(j) ) * ( longitude(j) - longitude(i) ) * ...
                                         cos( ( latitude(i) + latitude(j) ) / 2 ) + ...
                       ( vy(i) - vy(j) ) * ( latitude(j) - latitude(i) ) ) / ...
                  abs( ( vx(i) - vx(j) ) * ( alongtrack(i) * vx(i) - alongtrack(j) * vx(j) ) +
...
                       ( vy(i) - vy(j) ) * ( alongtrack(i) * vy(i) - alongtrack(j) * vy(j) ) );
      if endlap_ > 0
        % include sidelap only when the endlap exists
        count = count + 1;
        sidelap(count) = 1 - radius * ...
                         abs( ( vy(i) - vy(j) ) * ( longitude(j) - longitude(i) ) * ...
                                                cos( ( latitude(i) + latitude(j) ) / 2 ) -
...
                              ( vx(i) - vx(j) ) * ( latitude(j) - latitude(i) ) ) / ...
                         abs( ( vx(i) - vx(j) ) * ( crosstrack(i) * vx(i) - crosstrack(j) *
vx(j) ) + ...
                              ( vy(i) - vy(j) ) * ( crosstrack(i) * vy(i) - crosstrack(j) *
vy(j) ) );
        line = [ '>< ' deblank( dataset(i,:) ) sprintf( '_%03u', scene_num(i) ) ' : ' ...
                       deblank( dataset(j,:) ) sprintf( '_%03u', scene_num(j) ) ' : ' ...
                 num2str( 100 * sidelap(count) ) '%' ];
        if sidelap(count) > 0
          fprintf( fid, '%s\n', line );
        else
          fprintf( fid, '%s !!! GAP !!!\n', line );
        end
      end
```

```
    end
  end
end

% Display final results

fprintf( fid, '\n%s\n\n', ident );
%fprintf( fid, 'Ground elevation: %g ft\n\n', elevation );

if exist( 'endlap' ) == 1
  fprintf( fid, '%d endlaps\n', length( endlap ) );
  fprintf( fid, 'Mean endlap : %f%%\n', 100 * mean( endlap ) );
  fprintf( fid, 'Std. dev.   : %f%%\n', 100 * std( endlap ) );
  fprintf( fid, 'Minimum     : %f%%\n', 100 * min( endlap ) );
  fprintf( fid, 'Maximum     : %f%%\n', 100 * max( endlap ) );
  fprintf( fid, 'Portion of endlaps smaller than %g%% : %f%%\n', ...
              100 * end_spec, 100 * length( find( endlap < end_spec ) ) / length( endlap ) );
else
  fprintf( fid, 'No endlaps\n' );
end

fprintf( fid, '\n' );
if exist( 'sidelap' ) == 1
  fprintf( fid, '%d sidelaps\n', length( sidelap ) );
  fprintf( fid, 'Mean sidelap : %f%%\n', 100 * mean( sidelap ) );
  fprintf( fid, 'Std. dev.    : %f%%\n', 100 * std( sidelap ) );
  fprintf( fid, 'Minimum      : %f%%\n', 100 * min( sidelap ) );
  fprintf( fid, 'Maximum      : %f%%\n', 100 * max( sidelap ) );
  fprintf( fid, 'Portion of sidelaps smaller than %g%% : %f%%\n', ...
              100 * side_spec, 100 * length( find( sidelap < side_spec ) ) / length( sidelap )
);
else
  fprintf( fid, 'No sidelaps\n' );
end

fclose( fid );
```